2010

Farnesoid X Receptor Modulation by Systematic Ligands of Translocator Protein (18KDA)

Linnea Elsa Anderson
University of Rhode Island

FARNESOID X RECEPTOR MODULATION BY SYNTHETIC LIGANDS OF TRANSLOCATOR PROTEIN (18KDA)

BY

LINNEA ELSA ANDERSON

A THESIS SUBMITTED IN PARTIAL FULFILLMENT OF THE REQUIREMENTS FOR THE DEGREE OF

MASTERS OF SCIENCE

IN

BIOCHEMICAL AND PHARMACEUTICAL SCIENCES

UNIVERSITY OF RHODE ISLAND

2010

MASTER OF SCIENCE THESIS

OF

LINNEA ELSA ANDERSON

APPROVED:

Thesis Committee:

Major Professor ______________________

____

____

____

DEAN OF THE GRADUATE SCHOOL

UNIVERSITY OF RHODE ISLAND

2010

ABSTRACT

The synthesis of bile acids is the major biological mechanism for cholesterol removal in the human body. Strict regulation of both cholesterol and bile acid levels is necessary to maintain a healthy balance and to prevent health problems. Bile acids are natural ligands for farnesoid x receptor (FXR), a nuclear receptor that controls gene expression for multiple proteins involved in maintenance of bile acid homeostasis. Many endogenous and exogenous chemical ligands have been found to activate FXR; chenodeoxycholic acid (CDCA) is the most well characterized endogenous ligand. This study identifies a synthetic indole-acetamide, FGIN-1-27, as a new FXR agonist. FGIN-1-27 is already a known ligand of the translocator protein 18 kDa (TSPO), a mitochondrial cholesterol transporter.

FXR regulates target gene transcription through binding to special inverted repeat-1 (IR-1) consensus DNA elements. Ligand binding to FXR was measured by inserting an IR-1 sequence upstream of a firefly luciferase detector gene that increased transcription of luciferase proportional to ligand binding in a human hepatoma cell line (HuH-7). Results show that FGIN-1-27 is a partial agonist of FXR that activates FXR alone at 10 μM, but decreases activation from CDCA at 100 μM when cotreated. Two other well-known ligands of TSPO, FGIN-1-43 and PK11195 were investigated also for their effects on FXR mediated transcription. Both compounds acted as antagonists, decreasing the activity of CDCA (100 μM) while showing no activation of FXR alone at 10 μM treatment.

Agonist ligand binding to FXR increases the expression of the target gene, bile salt export pump (BSEP), and another nuclear receptor, small heterodimer partner (SHP). Through real time RT-PCR DNA amplification of both genes, we found FGIN-1-27 treatment in HuH-7 cells and primary human hepatocytes increased both BSEP and SHP gene expression. Additionally, expression of cholesterol 7α-hydroxylase (CYP7A1), an enzyme involved in bile acid synthesis, is negatively regulated by FXR; we show that FGIN-1-27 decreased the expression of CYP7A1.

In addition to *in vitro* studies, we investigated *in silico* molecular modeling of the binding of these TSPO ligands to FXR and demonstrated that these synthetic compounds fit into the ligand-binding pocket of FXR with favorable energy measurements. We identified key amino acids involved in agonist ligand binding *in silico,* and through mutation assays we confirmed that H447 is the major amino acid responsible for FXR interaction with an agonist ligand.

Taken together, FGIN-1-27 binding to and modulating two of the proteins involved in bile acid synthesis indicates there is overlap in the role of TSPO and FXR. FGIN-1-27 and related indole-acetamides may be potential therapeutic drugs beneficial to populations with enzyme deficiencies that cause high cholesterol levels. Further investigation of the role of mitochondria in bile acid synthesis will lead to a better understanding of the regulation of cholesterol and bile acid homeostasis.

ACKNOWLEDGEMENTS

This thesis is dedicated to my parents

There are only two lasting bequests we can hope to give our children.
One of these is roots, the other, wings.

~ Hodding Carter

PREFACE

This thesis is in manuscript format as designated by the University of Rhode Island.

TABLE OF CONTENTS

LIST OF TABLES

LIST OF FIGURES

FARNESOID X RECEPTOR MODULATION BY SYNTHETIC LIGANDS OF TRANSLOCATOR PROTEIN (18KDA)*

Linnea E. Anderson[1,2], Ann M. Dring[1,2], Roberta S. King[1], Laura D. Hamel[1,2], Ruitang Deng[1], Stephen C. Strom[3] and Matthew A. Stoner[1,2]

From the [1]Department of Biomedical and Pharmaceutical Sciences, [2]Rhode Island IDeA Network of Biomedical Research Excellence, Center for Molecular Toxicology, College of Pharmacy, University of Rhode Island, Kingston, Rhode Island, 02881, USA and [3]Department of Pathology, University of Pittsburgh School of Medicine, Pittsburgh, PA, 15213, USA

Running Title: Modulation of FXR by TSPO ligands

Address correspondence to: Matthew A. Stoner, Ph.D., 41 Lower College Road, 125 Fogarty Hall, Kingston, RI 02881. Tel.: 401-874-4681; Fax: 401-87-5787; E-mail: mstoner@uri.edu

A condensed version of this manuscript will be submitted to the Journal of Biological Chemistry

*This publication was made possible by RI-INBRE Grant # P20RR016457 from the National Center for Research Resources (NCRR), a component of the National Institutes of Health (NIH), and its contents are solely the responsibility of the authors and do not necessarily represent the official views of NCRR or NIH. Additionally, normal human hepatocytes were obtained through the Liver Tissue Cell Distribution System (LTCDS), Pittsburgh, Pennsylvania, funded by NIH Contract #N01-DK-7-0004 / HHSN267200700004C. The authors gratefully acknowledge the laboratory of Dr. Curtis Omiecinski (The Pennsylvania State University, State College, PA) for the generous supply of multiple plasmid constructs.

1. INTRODUCTION

1.1 Cholesterol and bile acid homeostasis

Bile acids are natural emulsifiers of dietary lipids, cholesterol, and fat-soluble vitamins (1). They are secreted into the small intestine and ultimately control the amount of cholesterol that is absorbed from the diet. Accumulation of excess cholesterol in circulation, due to deficiencies in enzymes of cholesterol catabolism, poor health and diet, and other risk factors, can lead to atherosclerosis and coronary heart disease (2,3). If the excretion of bile acids is hindered, the liver will accumulate these cytotoxic substances that are normally effluxed to the gall bladder and eventually to the duodenum, leading to cholestasis (4). The synthesis of bile acids must be tightly regulated to maintain homeostasis between cholesterol and bile acid concentrations. In adult human liver, approximately 500 mg of cholesterol is converted into bile acids each day through multiple pathways involving 16 different enzymes (reviewed by Russell (1)). About 95% of bile acids are re-circulated throughout the body before returning to the liver, while the other 5% are removed from the body through fecal matter. The biosynthesis of bile acids makes up about 90% of all cholesterol catabolism, with the remaining 10% going to steroid hormone biosynthesis (1,5,6).

Bile acid synthesis occurs through two main pathways, the classic/neutral and the alternative/acidic, each of which is initiated by a cytochrome P450 enzyme (CYP)[1] (extensively reviewed in (1,5,7-9)). CYP enzymes are a special gene superfamily

[1] See complete list of abbreviations (section 6) page 51.

responsible for the metabolism of multiple xenobiotic and endogenous compounds (10,11). Of the 57 human CYP genes, only seven take part in bile acid biosynthesis (7). Six of the bile acid synthesis CYP enzymes are present on endoplasmic reticulum of eukaryotic cells, the seventh being found only inside the inner mitochondrial membrane (12). Nuclear receptors often regulate transcription of cytochrome P450 genes through negative feedback from accumulation of a substrate, such as bile acids and oxysterols (13,14).

Most bile acids (~90%) are produced in the liver through the classic pathway, initiated by the rate-limiting cholesterol 7α-hydroxylase (CYP7A1) microsomal enzyme that converts cholesterol to 7α-hydroxycholesterol (1,15). The remaining 10% of bile acids are synthesized through the alternative pathway initiated by mitochondrial sterol 27-hydroxylase (CYP27A1) in extrahepatic tissues (16,17) or cholesterol 24-α hydroxylase (CYP46A1) in the brain (18). The alternative pathway forms oxysterols that must be further converted into bile acids through 7α-hydroxylation (19). Cholesterol homeostasis must be maintained in the brain as in other tissues, but cholesterol cannot readily cross the blood brain barrier. To overcome this problem, CYP46A1 produces 24S-hydroxycholesterol, an oxysterol that can cross the blood brain barrier, and be further converted into bile acids in the liver via the oxysterol 7α-hydroxylase (CYP39A1) (20). The CYP27A1-initiated pathway forms predominantly [redacted]-hydroxycholesterol, which is 7α-hydroxylated by CYP7B1 (21). CYP27A1 is involved also in both pathways further downstream in ring modifications to oxidize and cleave the sterol side chain (1,19). The alternative pathway produces solely

chenodeoxycholic acid (CDCA), while the classic pathway produces both CDCA and cholic acid (CA) (8). The relative abundance of CA versus CDCA is ultimately regulated by sterol 12α-hydroxylase (CYP8B1) (7). Figure 1 illustrates both pathways of bile acid synthesis in a condensed version showing only intermediates produced directly by CYP enzymes.

Since strict enzymatic control is required to prevent bile acid or cholesterol accumulation, mutations of CYP enzyme genes can have potentially drastic consequences. CYP7A1 and CYP27A1 are two main CYP enzyme genes with mutations most often associated with cholesterol metabolic diseases and conditions. A homozygous mutation in CYP7A1 is associated with hypercholesterolemia, a condition of high total cholesterol and low-density lipoprotein cholesterol (LDL-C) concentrations accumulating in plasma, and accumulation of cholesterol in the liver with limited bile acid synthesis or excretion (22-24). Studies have shown that 40-60% of the Caucasian North American population are carriers of an A to C substitution polymorphism in the CYP7A1 promoter region producing a high LDL-C phenotype with a recessive CYP7A1 -/- mutation that is more prevalent in men (23,25,26). Some individuals with this substitution have been shown to be resistant to cholesterol-lowering 3-hydroxy-3methylglutaryl-coenzyme A (HMG-CoA) reductase inhibitors and experienced premature gallstones from bile acid accumulation (23). It is hypothesized that the inhibition of cholesterol synthesis by HMG-CoA reductase inhibitors would not significantly decrease total cytosolic cholesterol concentrations, therefore the increase in LDL receptor expression normally resulting from inhibition

of cholesterol synthesis, thus decreasing LDL-C in blood, would be limiting with little effect on lowering LDL-C concentrations (23).

Lower than normal CA concentration is often an indicator of CYP7A1 deficiency as a result of the classic pathway being absent with compensation by the acidic pathway that produces only CDCA (22); typically the ratio of CA to CDCA is 2:1 (7,22). In the event of this compensation, CYP27A1 activity doubles preventing complete deficiency of CYP7A1 from being lethal (23). Components of the acidic pathway can also be affected by mutations. Mutations that decrease CYP27A1 expression or activity lead to irregular cholesterol catabolism, and are involved in cerebrotendinous xanthomatosis (CTX), an inherited syndrome of neurological problems and premature atherosclerosis (27,28). The 40 known gene mutations that cause CTX are implicated in the build-up of cholestanol (a sterol cholesterol derivative) in myelin sheaths in the nervous system. If the disease is discovered early enough it is often treatable with oral bile acid therapy (1,5).

1.2. Role of translocator protein (18 kDa)

The acidic pathway is limited not by the initial enzyme CYP27A1 itself, but by the delivery of cholesterol to CYP27A1 in the mitochondria (29). The transport of cholesterol into the mitochondria occurs through the translocator protein 18 kDa (TSPO), which is located predominantly on the outer mitochondrial membrane (OMM) (30,31) in cells of the adrenal glands, lung, heart, liver, and multiple other tissues (32). TSPO possesses five membrane-spanning domains that can form

multimeric protein polymers able to bind endogenous ligands that facilitate cholesterol binding (31,33). The polymer formation is facilitated by reactive oxygen species most likely produced from the CYP enzyme activity inside the mitochondria (31). TSPO, however, does not act alone and requires the assistance of steroidogenic acute regulatory (STAR) protein (34) (Fig. 2). Through a complex pathway, cholesterol binds to STAR in the cytoplasm for transport to the mitochondria (35), then STAR binds to the OMM (36), where cholesterol can be transported to TSPO and mobilized across the outer to the inner mitochondrial membrane. Binding of ligands to TSPO, including the endogenous ligand, diazepam-binding inhibitor, allows cholesterol to be transported into the mitochondrial, (37-39). Both endogenous and exogenous ligands increase 27-hydroxycholesterol production, identifying the availability of cholesterol to CYP27A1 as the rate-limiting step in the alternative pathway (40).

1.3 Role of nuclear receptors

In high concentrations, bile acids can be toxic, so the potential toxicity is regulated by negative feedback (41). Bile acid synthesis is reduced in the presence of high bile acid concentrations, and conversely, low concentrations result in bile acid synthesis activation to increase the bile acid pool (1). Bile acid feedback is regulated by nuclear receptors that directly control target genes by activating or repressing transcriptional activities. Typically, nuclear receptors have a DNA binding domain that recognizes specific DNA sequences (hormone response elements) through a zinc finger region, and a ligand-binding domain (LBD). The response elements are comprised of half-sites at least 6 base pairs long (typically AGGTCA) (42,43). Nuclear receptors bind to

response elements as either a homo/heterodimer to sequences of direct (DR) (→→), everted (ER) (←→) or inverted (IR) (→←) repeats spaced by 1-5 nucleotides, or as a monomer, binding only to a half site (44). Helix 12 of the LBD is a ligand dependent activation function-2 (AF-2) domain, which upon agonist ligand binding to the receptor will recruit a coactivator protein with acetyltransferase activity (43). Acetylation of residues on histone proteins causes relaxation of the chromatin structure so the transcriptional machinery can gain access to the DNA to increase gene transcription (45).

The endogenous bile acid receptor, farnesoid x receptor (FXR; NR1H4), a member of the nuclear receptor superfamily (46), is a good potential target for pharmacological therapy to regulate bile acid concentrations, and thus cholesterol concentrations. FXR forms an exclusive heterodimer with retinoid x receptor α (RXRα; NR2B1) (47) (the heterodimer formation occurs independent of ligand and DNA binding, but it is necessary for FXR receptiveness to bile acid ligand binding (47,48)). Multiple studies show that the primary and secondary bile acids: CDCA, lithocholic acid, and deoxycholic acid, are endogenous ligands of FXR, which in turn regulate bile acid homeostasis through transcriptional effects on specific genes (49-51). The most potent endogenous ligand of FXR is CDCA (50,51) and CDCA binding to FXR recruits the steroid receptor coactivator-1 (SRC-1) to the LBD (46,50,51). Along with bile acids, potent exogenous ligands of FXR have been made, including the potent synthetic agonists GW4064 (52), fexaramine (53) AGN29 and AGN31 (54). Additionally,

guggulsterone, a compound isolated from the guggul tree traditionally used in Ayurvedic medicine, is a natural antagonist of FXR (55).

Agonist ligands of FXR play a major role in feedback regulation of bile acid synthesis. FXR can indirectly repress CYP7A1 expression through an FXR-activated small heterodimer partner (SHP; NR0B2) pathway (56). FXR binds to an IR-1 repeat on the promoter region of SHP increasing SHP transcription and expression (57). SHP then interacts with other nuclear receptors, either liver receptor homolog-1 (LRH-1; NR5A2) (58,59) or hepatic nuclear factor-4 (HNF4; NR2A1) (60), by competing for coactivators, recruiting corepressors, or through its own intrinsic corepressor function (61). LRH-1 binds as a monomer to the promoter region of CYP7A1 gene (5'-TCAAGGCCA-3') (56,62), while HNF4 binds as a homodimer to a DR-1 response element (5'-TGGACT T AGTTCA-3') (63). FXR is known also to increase bile acid efflux from the liver. FXR binds to an IR-1 repeat (5'-GGGACA T TGATCCT-3') on the promoter region of the gene for bile salt export pump (BSEP), an ATP-mediated receptor on the bile canaliculi, increasing its expression (64). The liver specific BSEP is the principal bile acid efflux transporter that pumps bile acids against a strong concentration gradient out of the liver; precise control of this receptor is essential for maintenance of bile acid homeostasis (65,66).

In most cases, agonist activation of FXR should lower cholesterol up-take by diminishing the liver bile acid pool through increased efflux and through inhibition of CYP7A1 activity, thereby inhibiting cholesterol absorption in the intestine (67).

However, this is not always the case since FXR agonists would show little effect in people lacking functional CYP7A1 enzymes. Also, CYP27A1 is not a rate-limiting enzyme, so bile acids and their intermediates have less effect on this pathway in comparison to CYP7A1; agonist effects of FXR through bile acids typically do not regulate transcriptional activity of CYP27A1 directly (68,69). Individuals with poor synthesis via the classic pathway, therefore, may therapeutically benefit from relevant and useful targets of TSPO as a modulator of the alternative pathway.

1.4. TSPO and FXR interplay

It is possible that many of the known ligands of TSPO could additionally regulate the cholesterol turnover rate by acting upon other receptors. Since both mitochondrial and nuclear receptor signaling pathways are involved in maintenance of bile acid homeostasis, this study was designed to investigate the interplay between TSPO and FXR by demonstrating TSPO ligands modulate FXR activity also. PK11195, one of the most well known and widely used ligands of TSPO, is known to increase the cholesterol binding rate to the protein (31,70,71). Similarly, a series of 2-aryl-3-indoleacetamides (named FGIN-1), designed by Romeo et al. (72), selectively bind to TSPO (73,74). The aim of this study was to investigate binding of PK11195 and FGIN-1 compounds to modulate FXR target genes and to provide evidence of binding pocket interactions with these compounds. We have found that FGIN-1-27 is a partial agonist of FXR that activates downstream transcription of FXR target genes, as demonstrated in both optimized luciferase assays and measurements of endogenous gene expression in liver cells. We show that FGIN-1-43 is a selective antagonist, able

to block FXR agonist activation of FGIN-1-27 but is less inhibitory of CDCA activation of FXR. PK11195, on the other hand, is a non-selective FXR antagonist. Through *in vitro* transcriptional and mRNA expression studies and *in silico* molecular modeling studies we show that each of these compounds binds directly to the FXR LBD. Activation of both TSPO and FXR with one compound is favorable for dual maintenance of bile acid and cholesterol homeostasis.

2. EXPERIMENTAL PROCEDURES

2.1. Chemicals and biochemicals

CDCA (sodium salt) was purchased from Sigma-Aldrich® (St. Louis, MO). FGIN-1-27, FGIN-1-43, and PK11195 were purchased from Tocris Bioscience (Ellisville, MO). Dimethyl sulfoxide (DMSO), used as a negative control with all treatments, was purchased from Fisher Scientific (Pittsburgh, PA). The γ-aminobutyric acid (GABA)-ergic ligand library (version 3.6, lot # N1205) was purchased from Biomol (now Enzo Life Sciences, Plymouth Meeting, PA). Cell culture media and additives were from Invitrogen/GIBCO Corp. (Carlsbad, CA) or Lonza (Hopkington, MA).

2.2. Plasmid constructs

Consensus FXR response element (FXRE) (75) contained four copies of the IR-1 sequence (underlined) 5'-ACAAGAGGTCATTGACCTTGTCC-3'. Forward and reverse oligonucleotides of the IR-1 sequence were annealed and blunt-end ligated into the *Sma I* site of luciferase vector pTK-Luc. To make pTK-Luc, pGL3-Basic vector (Promega, Madison, WI) was cut with *BglII* and blunted with T4 polymerase. A DNA fragment (165 bp) containing the core thymidine kinase (TK) promoter was cut from vector pBLCAT2, blunted with T4 polymerase and ligated into pGL3 vector maintaining the original multiple cloning site. Original pTK-Luc and FXRE-TK-Luc cloning was performed in the laboratory of Dr. Curtis Omiecinski (The Pennsylvania State University, State College, PA). Expression plasmids for FXR were produced in pcDNA3.1 vector (Invitrogen/GIBCO), p3XFLAG vector (Sigma Aldrich) and pM

vector (BD Bioscience, San Jose, CA). Human liver cDNA was subjected to PCR amplification of FXR gene using gene-specific primers (FP: 5'-CGCGGATCCTAGCCGCCATGGGATCAAAAATGAATCTC-3' and RP: 5'-GCTCTAGATCACTGCACGTCCCAGATTTCA-3'); primers were designed to amplify cDNA coding for the full 472 amino acid FXR sequence (NM_005123). FXR PCR product and vector were separately digested with *BamHI* and *XbaI* before being combined for ligation. For a mammalian two-hybrid assay, the reporter vector, pFR-Luc, containing five copies of an upstream activation sequence (UAS) that binds to GAL4 protein (76), was cloned upstream of the firefly luciferase gene. pVP16-FXR contained the full-length FXR cloned downstream of, and fused to, VP16 activation function. GAL4-containing plasmid pM-SRC-1 was made by PCR amplification of SRC-1 sequence coding for amino acids 570-780 (contains one of the receptor interacting domains (RID)) using the following primers, based on gene accession number NM_003734: FP: 5'-GATCGAATTCCCTAGCAGATTAAATATACAA CCAG-3' and RP: 5'-GATCTCTAGATCACATCTGTTCTTTCTTTTCCACTT-3'. PCR-amplified product was digested with *EcoRI* and *XbaI* for cloning into pM.

2.3. Cell culture

HuH-7 cells (JTC-39), a differentiated hepatoma cell line, were originally from Okayama University JCRB Cell Bank and kindly provided by Dr. Ruitang Deng, University of Rhode Island, Kingston, RI. COS-1 cell line (African Green Monkey kidney cells transformed with Simian Virus 40) and ZR-75 (breast cancer cell line) were obtained from American Type Culture Collection (ATCC, Manassas, VA). HuH-

7 and COS-1 cells were maintained in Dulbecco's Modified Eagle Medium (DMEM) supplemented with 5% fetal bovine serum (FBS), 1% penicillin/streptomycin, 1% Glutamax, and 0.15% sodium bicarbonate, 1% sodium pyruvate, 10 mM HEPES buffer, and 1% non-essential amino acids (Invitrogen/GIBCO). ZR-75-1 cells were maintained in RPMI 1640 medium with 10% FBS and the same concentrations of additives as for DMEM. Additionally, primary human hepatocytes were obtained from an NIH-funded liver tissue cell distribution system (LTCDS) through Dr. Steven Strom at the University of Pittsburgh (Pittsburgh, PA). The human hepatocytes were seeded onto collagen type IA-coated culture plates and maintained with Williams' Media E medium supplemented with isulin-transferrin-selenium (ITS+) solution, 100 nM dexamethasone, linoleic-bovine serum albumin conjugate, penicillin/streptomycin and L-glutamine additives (77). Hepatocyte maintenance medium was changed every other day and experiments were performed within 1-2 weeks after cell arrival to the lab.

2.4. Transient transfections

2.4.1. HuH-7 transfections with FXRE response element

T_{25} flasks of HuH-7 cells were transiently transfected with 5 μg of $p(FXRE)_4$-TK-luc reporter plasmid and 0.5 μg of *Renilla* luciferase expression plasmid (pRL-CMV) (Promega), using FuGeneHD transfection reagent (Roche, Brandford, CT), Lipofectamine2000 transfection reagent (Invitrogen/GIBCO) or Polyethylenimine (PEI) with an average MW of 25 kDa (Polysciences, Inc, Warrington, PA); a 1mg/mL stock solution of PEI was made in 20 mM HEPES buffer. The following transfection

reagent ratios (μL reagent: μg DNA) were used for each type of transfection: FuGeneHD (3:1), Lipofectamine2000 (3.5:1), or PEI (4:1). Transfections were performed in serum-free media for 6-24 hours. In addition to the reporters, 1.25-2.5 μg of emerald green fluorescent protein (pEGFP-Cl) (Clontech, Mountain View, CA) was transfected into the cells to monitor transfection efficiency. Transfected HuH-7 cells were then trypsinized and re-seeded into a 96-well plate and treated for 24 hours. The 60 GABA-ergic compounds (Table 1) were screened using single-well treatments. Cotreatments of CDCA with FGIN-1-27, FGIN-1-43, and PK11195 were balanced with equal amounts of solvent control, DMSO. Luciferase activity was measured using Dual-Glo Luciferase Reporter kit (Promega) on a GloMax 96 Microplate Luminometer (Promega). The luminescence from the firefly luciferase was normalized to the Renilla luciferase luminescence to control for transfection efficiencies and for well-to-well variation in cell numbers. The ratios of the measurements were calculated and reported as mean fold change relative to DMSO (control) ± standard error of the mean (SEM) (when greater than two replicates were performed).

2.4.2. Exogenous FXR expression

For exogenous expression of FXR in HuH-7 and ZR-75-1 cells, 1.25 μg of 3.1-FXR was transfected along with p$(FXRE)_4$-TK-luc, *Renilla*, and pEGFP-Cl. As a control, cells were also transfected with 1.25 μg of pcDNA3.1(+) empty vector in place of 3.1-FXR.

2.4.3. Mammalian two-hybrid assay

T_{25} flasks of COS-1 cells were transfected with 5 μg pFR-Luc reporter plasmid, 1.5 μg of pM-SRC-1 construct, 1.5 μg of VP16-FXR LBD, 0.5 μg pRL-CMV, and 1.5 μg pEGFP-Cl. Transfected COS-1 cells were trypsinized then re-seeded into 96-well plates, treated, and luminescence measured using Dual-Glo, as described in section 2.4.1.

2.4.4. FXR Mutants

Point mutations of single amino acids of FXR, generously provided by Dr. Ruitang Deng, were formed using a QuikChange site-directed mutagenesis kit (78,79). The mutation sequences are listed in Table 2. ZR-75-1 cells were seeded into 6-well plates and transiently transfected with 1 μg $p(FXRE)_4$-TK-luc, 100 ng pRL-CMV, 200 ng pEGFP-Cl, and 500 ng of 3.1(+), 3.1-FXR, or hFXR mutant per well. The cells were trypsinized and each well of a 6-well was re-seeded into a portion of a 96-well plate, treated for 24 hours and read on the Microplate Luminometer, as described in section 2.4.1.

2.5. Real-time RT-PCR

HuH-7 cells were seeded into 12-well plates and each well was treated with a different compound for 24 hours. Similarly, the human hepatocytes were obtained in 12-well plates and treated after 4-6 days of routine maintenance. Following the protocol from Invitrogen/GIBCO, total RNA was harvested from the cells using TRIzol reagent. The RNA was reverse transcribed into cDNA using a High Capacity cDNA Reverse

Transcription kit (Applied Biosystems, Carlsbad, CA). cDNA was subjected to gene-specific amplification of FXR target genes using SYBR Green PCR Master Mix (Applied Biosystems). Reactions were made 50 μL at a time with 25 μL of 2x SYBR Green PCR master mix, 21 μL of nuclease free water, 1 μL each of the 10 μM forward and reverse primers, and 2 μL of cDNA (4 ng/μL). The actin, BSEP, CYP7A1, FXR, HNF4α, and LRH-1 primers were from Eurofins MWG Operon (Huntsville, AL), and RXRα primers were from Integrated DNA Technologies (Coralville, IA) (see sequences in Table 3). Each 50 μL reaction was split into 2 wells in a 96-well plate to provide technical replicates. RT-PCR SYBR Green amplification was performed using a 7500 Real-Time PCR System from Applied Biosystems with thermocycling as follows: 2 minutes at 50°C, 10 minutes at 95°C, followed by 40 cycles of 95°C for 15 seconds and 60°C for 1 minute. All values were normalized to actin, due to its ubiquitous and constant expression in all cells, and were reported as fold change relative to mean DMSO (control) ± SEM. Applied Biosystems v2.0 SDS software was used for analysis; auto threshold and auto baseline settings were used to ensure that the optimum analysis settings were used for all reactions. Threshold values were set in the exponential phase of the change in normalized reporter dye fluorescence (ΔR_n). The baseline of each sample was set to eliminate background noise from the measurements.

2.6. Molecular modeling

To further investigate the docking of compounds in the LBD of FXR, *in silico* molecular modeling with Scripps Research Institute's (La Jolla, CA) AutoDock v4.2

was performed on CDCA, PK11195 and several FGIN-1 compounds. The crystal structure of FXR was obtained from the Protein Data Bank (PDB.org) (PDB ID code 3BEJ) (80). The structure had 237 residues (amino acids 235-472) of the LBD crystallized with Merck FXR agonist #1 (MFA-1) that occupied the pocket in an active conformation, with a small fragment of SRC-1 (residues 676-700) that was bound to the AF-2 domain (helix 12) of FXR. The coordinates for residues 235-243 and 472 of FXR were missing and not accounted for.

Using Discovery Studio Visualizer v2.5 (Accelrys, San Diego, CA) the protein crystal structure was inspected and cleaned of any misplaced or misinterpreted atoms. Polar hydrogens were added to each amino acid to complete the valance of each atom (non-polar hydrogens were implied). The valence of charged amino acids was adjusted so the overall charge on each residue was an integer, e.g. the guanidine group on arginine was given two hydrogens per nitrogen so a neutral charge resulted. Since the protein was only a portion of FXR, the end residues were adjusted to mimic the N-terminal and C-terminal for the purposes of docking. The N-terminal nitrogen of Glu244 was allowed two hydrogens to make a +1 charge and the C-terminal Val471 was given a hydroxyl group to complete the carboxylic acid to make a -1 charge. These changes allowed the polar hydrogens and gasteiger charges to be added to the protein without errors in AutoDock Tools v4.2 (ADT). Polar hydrogens were added to the 3D coordinates of the ligand chemical structures generated from SMILES strings in Discovery Studio. One of the main advantages of AutoDock was that full ligand flexibility was possible for docking to static or partially flexible macromolecules (81).

For compounds in this study, the number of torsions were as follows: FGIN-1-27, FGIN-1-43, FGIN-1-51 all had 14 torsions, FGIN-1-20 had 8 torsions, PK11195 had 5 torsions, and CDCA had 7 torsions. A grid box was positioned over the ligand-binding pocket with a box size of 50 x 36 x 36 with one grid unit equal to 0.375 Å. Map files were formed for each atom type within the ligand (all contained different heteroatoms O, F, Cl, N) with the FXR LBD structure using AutoGrid. This file contained the position characteristic of every atom so the grid map calculations were represented for each ligand.

Each ligand was started in a random position within the grid box. The Lamarckian genetic algorithm parameters were as follows: genetic algorithm (GA) runs (100 or 200), population size (150), maximum number of evaluations (2,500,000), and maximum number of generations (27,000). The local search parameters were as follows: number of local search runs (50), maximum number of iterations (300), and probability of any particular phenotype being subjected to local search (0.01). To allow for accurate energy calculations, the number of evaluations must increase for the number of ligand torsions. Increasing the number of GA runs with 2,500,000 evaluations per run allowed for more accurate calculations. Due to computational constraints, the GA runs were performed 100 or 200 runs at a time, 800 total for the FGIN-1 compounds and 600 total for CDCA and PK11195, the resulting docking log files were then combined by opening groups together in ADT and reclustering at 2.0 Å root-mean-square (RMS). Clusters containing fewer conformations than the determined random number value were disregarded (calculation: # GA runs / # of

clusters = random value). Therefore, clusters that contained very few conformations were more likely formed by random chance. Average binding energies for each cluster not formed at random were calculated and graphed as histograms. The conformations with the lowest binding energies were evaluated for possible hydrogen bonding using Discovery Studio's hydrogen bond monitor default parameters. Additionally, van der Waals interactions were measured using the intermolecular neighbor monitor in Discovery Studio. The distance between atoms in each residue and each ligand were further analyzed. The van der Waals interactions were calculated by addition of the radii of atoms in the ligand and surrounding amino acid atoms with the following radii values: carbon-1.87Å, nitrogen-1.50 Å, oxygen-1.40 Å, hydrogen 1.10 Å, fluorine-1.47 Å, chlorine-1.75 Å, and sulfur-1.85 Å.

2.7. Statistical analysis

Individual values of luciferase assay replicates were analyzed using Student's t-test. The mean, SEM, n values were used to determine significance of RT-PCR values also using Student's t-test. A Grubbs' outlier test was used on all replicate values prior to mean calculations. Differences were deemed statistically significant differences where $p \leq 0.05$.

3. RESULTS

3.1 TSPO ligands bind also to FXR

3.1.1 GABA-ergic library screen

Since many chemical compounds bind to both GABA receptors and TSPO, we screened a GABA-ergic chemical library (compounds are listed in Table 1), which contained specific TSPO ligands (F series), to examine the overlapping involvement of TSPO ligands binding also to FXR. In this screening assay, agonist ligand binding to FXR drove the expression of an IR-1 regulated luciferase reporter gene. In the library screen (Fig. 3A), one compound, F2 (FGIN-1-27), increased luciferase expression considerably compared to the control. This increase was similar to that observed with CDCA treatment. Conversely, two compounds structurally similar to FGIN-1-27 that are TSPO ligands also, FGIN-1-43 (F3) and PK11195 (F10), did not increase luciferase expression. Since the FGIN-1 compounds were previously shown to be a selective ligand of TSPO (73,74) and PK11195 is a known ligand (31,70,71), these compounds were still included in further experiments for comparison. The chemical structures of the FGIN-1 compound contain the same 2-aryl-indole-3-acetamide backbone with varying halide substitutions and hydrocarbon tail lengths. PK11195 has similar aryl ring structures to the FGIN-1 compounds with chlorine on the phenyl ring. These compounds are quite structurally different from CDCA as seen in Figure 3B (the carbons of CDCA are numbered to correspond with the text).

3.1.2. Coactivator recruitment

One indicator that a compound is a ligand of a nuclear receptor is their ability to recruit coactivators. In the presences of an agonist ligand, the histone acetyltransferase, SRC-1, is recruited to the LBD of FXR (82,83). To further validate that these compounds bind to FXR, a mammalian two-hybrid assay was used to demonstrate coactivator recruitment to a ligand-activated FXR (Fig. 4). CDCA at 10 μM and 100 μM significantly increased luciferase expression compared to the control, signifying coactivator recruitment. Similarly, FGIN-1-27 at 5 μM and 10 μM also significantly recruited SRC-1 to the LBD. FGIN-1-27 displayed maximum agonist activity at 5 μM - 10 μM. Interestingly, PK11195 significantly decreased luciferase expression compared to the control, indicative of decreased basal SRC-1 recruitment.

3.2. HuH-7 hepatoma cell line expresses endogenous FXR

Human hepatocytes are the ideal cell type for *in vitro* studies of liver pathology and physiology studies, but cannot be easily obtained in large numbers because of limited availability of healthy donors. Therefore, we examined two cell lines as alternatives to primary hepatocytes. Our results showed that the HuH-7 cell line expressed similar amounts of endogenous FXR mRNA compared to human hepatocyte case HH1498 (Fig. 5A). ZR-75-1 breast cancer cell line, on the other hand, expressed very little FXR compared to HH1498. ZR-75-1 was chosen as a good cell line to use for FXR over-expression studies that required limited endogenous FXR interference. All cell lines tested expressed similar amounts of RXRα, with no significant difference compared to HH1498. HuH-7 cells expressed very little endogenous SHP but did not

lack LRH-1 or HNF4α expression (Fig. 5B). In HuH-7 cells, both CDCA and FGIN-1-27 significantly increased IR-1 driven luciferase expression in the presence and absence of exogenous FXR (Fig. 5C), while FGIN-1-43 did not modulate luciferase activity. There was a significant increase in luciferase expression when ZR-75-1 cells were treated with CDCA and FGIN-1-27 in the presence of exogenous FXR (Fig. 5D). No change occurred from treatments in the ZR-75-1 cells in the absence of exogenous FXR.

3.3. FGIN-1-27 is a partial agonist of FXR; PK11195 and FGIN-1-43 are antagonists

To further explore the binding of TSPO ligands to FXR, we examined the effects of FGIN-1-27, FGIN-1-43 and PK11195 on CDCA-activated FXR. Figure 6 represents the binding properties of these compounds in different combinations of treatments at varying concentrations. As expected, CDCA and FGIN-1-27 increased luciferase expression alone at all concentrations. Our study showed that FGIN-1-27 (10 μM), FGIN-1-43 (10 μM) and PK11195 (10 μM and 1 μM) decreased luciferase expression of CDCA-activated FXR at 100μM. However, when CDCA was limiting (≤ 10 μM), FGIN-1-27 further activated FXR and exhibited an additive effect with CDCA. When CDCA was at 100 μM, FGIN-1-27 (10 μM) significantly decreased transcription, acting as a partial agonist. Additionally, FGIN-1-43 (10 μM) antagonized CDCA at 100 μM and was not an agonist alone. When CDCA concentration was limiting, FGIN-1-43 had no effect on CDCA-activated FXR; however, FGIN-1-43 (10 μM) did decrease luciferase expression due to FGIN-1-27 agonist effects at 10 μM and 1 μM. PK11195 (10 μM) decreased FXR activation by CDCA at 100 μM, 10 μM, 1 μM and

100 nM. PK11195 alone significantly decreased basal transcription levels at 10 μM. Additionally, PK11195 at both 10 μM and 1 μM decreased FGIN-1-27-activated (1 μM and 10 μM) luciferase expression.

3.4. Effect of compounds on genes downstream of FXR

3.4.1 Changes in BSEP and SHP expression

Another way to measure transcriptional effects of a compound on a nuclear receptor is to look at regulation of specific downstream target genes. FXR ligands directly increase transcription of downstream genes, including BSEP and SHP (84). In our studies, FGIN-1-27 increased mRNA expression of both BSEP and SHP in human hepatocytes (cases HH1486 and HH1498) and HuH-7 cells similar to levels seen with CDCA treatment, while FGIN-1-43 did not increase basal expression(Fig. 7 and 8). Cotreatments of FGIN-1-43 or PK11195 with CDCA and FGIN-1-27 did not significantly decrease BSEP mRNA expression in HH1498 (Fig. 7); however, similar to the luciferase FXRE results in HuH-7 cells, FGIN-1-43 did significantly repress BSEP and SHP expression induced by FGIN-1-27 ligand binding, but not CDCA. PK11195 did not repress CDCA or FGIN-1-27 induced BSEP mRNA expression in HuH-7 cells or in HH1498. Conversely, FGIN-1-43 and PK11195 increased SHP mRNA expression when combined with CDCA in HH1498 (Fig. 8). PK11195 also increased SHP expression when combined with FGIN-1-27 in HH1498. In HH1498, PK11195 alone increased mRNA expression of both BSEP and SHP.

3.4.2. Changes in CYP7A1 expression

Another downstream target gene of FXR is CYP7A1, though the gene is indirectly regulated; CDCA indirectly represses CYP7A1 expression through a SHP mediated pathway (56). Results show that both CDCA and FGIN-1-27 significantly repress CYP7A1 expression in human hepatocytes (Fig. 9). FGIN-1-43, on the other hand, does not alter basal expression of CYP7A1. Unfortunately, CYP7A1 expression studies in HuH-7 cells yielded inconsistent results (data not shown), most likely due to the low expression of SHP (Fig. 5B). In another study, we also showed that PK11195 significantly repressed CYP7A1 expression in HH1498, but to a lesser extant than the effects seen by CDCA and FGIN-1-27 (Fig. 9).

3.5. TSPO ligands bind to the LBD of FXR

To further explore the capacity of PK11195 and 4 FGIN-1 compounds to fit into the LBD of FXR, *in silico* molecular modeling was performed. Docking results verified that these TSPO ligands could fit into an active conformation of FXR. The crystallized structure of human FXR (PDB ID code 3BEJ) (80) was used as the template to study the binding properties of CDCA, PK11195, and 4 FGIN-1 compounds. This template was among 9 crystallized structures of FXR in the PDB, all of which had a ligand and coactivator bound, except for 1OSH, which lacked a coactivator. Although this template has been used for other docking experiments (78), 1OSH also lacked a significant portion of helix 3, and therefore was not an ideal candidate. Two of the structures were isolated from rat FXR, differing from human FXR by only 12 amino

acids, but for the purpose of this study, only human FXR was relevant. Of all of the human crystallized structures, 3BEJ chain B was the most complete structure with the lowest b-factors in the binding pocket, so it was the best choice. B-factors are a measure of the disorder in the x-ray diffraction pattern caused by temperature-dependent vibrations, and so provide a measure of confidence in the accuracy of each atom's coordinates. MFA-1 formed an active conformation in the crystal structure, co-crystallized with a 24 amino acid fragment of SRC-1 bound to helix 12 of FXR (80) (Fig. 10). For each theoretical conformation generated by AutoDock, an estimate of the free energy of binding was calculated by the following formula: [final intermolecular energy (van der Waals, H-bond, desolvation energy + electrostatic energy)] + [final total internal energy] + [torsional free energy] – [unbound system's energy]. The lower the free energy of binding, the more energetically favorable the conformation.

3.5.1. Docking of CDCA

CDCA was allowed to have seven rotatable bonds so only 600 GA runs were necessary to reach a state of no further refinement. At 2.0 Å RMS clustering restraints, ADT formed eight conformational clusters with estimated free energy of binding ranging from -10.43 kcal/mol to -8.51 kcal/mol. The majority of conformations fell into two of the eight conformational clusters; the other 6 contained fewer conformations than the random number value (600/8 = 75) so they were disregarded from further analysis. The largest cluster contained 493 conformations with an average binding energy of -9.75 ± 0.009 kcal/mol (conformation *a*). The second largest cluster

had 75 conformations with an average binding energy of -9.45 ± 0.028 kcal/mol (conformation *b*) (Fig. 11A). Conformation *a* oriented the carboxyl group on C24 of CDCA near T288 to form hydrogen bonds (hydroxyl oxygen 2.39 Å, hydroxyl hydrogen 1.88 Å, carboxyl oxygen 1.77 Å). In a flipped orientation (conformation *b*), the CDCA carboxyl group hydrogen bonded to Arg331 (2.16 Å) and the oxygen of C7 hydrogen bonded to H447 (2.20 Å). Not surprisingly, CDCA in conformation *a* fit an orientation similar to MFA-1 (Fig. 10), which is a CDCA analog with an additional phenyl ring at C21 and a carboxyl group at C3 (80). Results show CDCA in both conformations was able to form van der Waal interactions with 13 residues on helices 3, 5, 10/11 and 12.

3.5.2. Docking of FGIN-1-27

Although structurally quite different from CDCA, FGIN-1-27 is a very hydrophobic molecule and also fit into the ligand-binding pocket of FXR with inhibition constants in the nanomolar range. From 800 GA runs, where free energy of binding ranged from -10.23 kcal/mol to -5.80 kcal/mol, ADT formed 102 conformational clusters at 2.0 Å RMS clustering restraints, 77 of which contained fewer conformations than the random number value (800/102 = 7.8), so were most likely reflected background noise. Although AutoDock 4.2 allows flexible ligand docking to bind to a fixed protein, increasing ligand flexibility (> 10 torsional degrees of freedom) decreases consistency of the conformation clusters (81). FGIN-1-27 was fully flexible with 14 torsional bonds that rotated freely, compared to CDCA, which only had seven. This, in part, explained the greater number of clusters generated despite the greater number of

GA runs. Closer inspection of the conformational clusters revealed that many clusters shared similar positions of the core ring structure, with the majority of variations between clusters being accounted for by the numerous positions adopted by the flexible hydrocarbon tails. For the FGIN-1 compounds, additional analysis was performed to identify four major conformations based upon position of the core ring structure only. As seen in Figure 11B, of the 25 non-random clusters of FGIN-1-27, 41% represented conformation *a,* where fluorine formed a hydrogen bond with T288 (1.97 Å). One study showed that fluorine attached to an aromatic carbon can form a hydrogen bond when the protein's donor atom is at an average distance of 2.698 Å (85). 20% of the clusters (conformation *b*) positioned fluorine close enough to hydrogen bond to Y369 (2.44 Å). The other two conformations (20% *c* and *18% d*) oriented the rings perpendicular to the pocket. Similar to CDCA, FGIN-1-27 was most likely held in place in the LBD by van der Waals interactions with 16-18 residues on helices 3, 5, 6, 7, 10/11, and 12.

3.5.3. Docking of FGIN-1-20

Analogs of FGIN-1-27 were also docked into FXR to examine the significance of fluorine and the hydrocarbon tails to the binding properties. When the hydrocarbon tails were shortened from hexyls to propyls in FGIN-1-20 (Fig. 11C), the number of torsions decreased by 6, resulting in fewer overall conformational clusters. From 800 GA runs of FGIN-1-20, free energy of binding ranged from -9.64 kcal/mol to -7.79 kcal/mol. ADT formed 35 conformational clusters at 2.0 Å RMS clustering restraints,

28 of which contained fewer conformations than the random number value (800/35 = 22.9). Similar to FGIN-1-27, fluorine in conformation *a* hydrogen bonded to T288 (1.94 Å) but with an increased occurrence of 60%. The shorter tails limited FGIN-1-20 from fitting into conformation *b* and favored conformation *c* at 34%. Additionally, the oxygen in conformation *c* formed a hydrogen bond with H447 (2.14 Å). FGIN-1-20 had lower average binding energies for each cluster compared to FGIN-1-27. No conformation *d* was formed. FGIN-1-20 still interacted with 13 amino acids of helices 3, 5, 6, 7, and 10/11, which were most likely allowed for hydrophobic interactions.

3.5.4. Docking of FGIN-1-51

The loss of the fluorine in FGIN-1-51 (Fig. 11D) caused no difference in orientation compared to FGIN-1-27, and had a similar binding fingerprint. FGIN-1-51 was run 800 times and reclustered at 2.0 Å RMS clustering restraints forming 111 conformational clusters. Free energy of binding ranged from -10.44 kcal/mol to -6.52 kcal/mol. Of these 111 clusters, 24 contained fewer than the random number value (800/111 = 7.2) of conformations so they cannot be distinguished from background. FGIN-1-51 favored conformation *b* and decreased the overall average binding energies per cluster compared to FGIN-1-27 and FGIN-1-20. The absence of fluorine, however, prevented FGIN-1-51 from forming hydrogen bonds with any of the residues in the LBD.

3.5.5. Docking of FGIN-1-43

The structure of FGIN-1-43 differed from FGIN-1-27 only by lacking fluorine and

possessing two chlorines. FGIN-1-43 also was allowed 14 torsions so 800 GA runs were necessary. The range of free energy of binding values was much larger than for any of the other FGIN-1 compounds, from -12.30 kcal/mol to -1.55 kcal/mol. From first evaluations, 152 conformational clusters were formed; 116 contained fewer than the random number value (800/152 = 5.3) of conformations so they were considered to be background and unlikely to be significant. FGIN-1-43 in Figure 11E had similar orientations to FGIN-1-27 but showed a greater range of binding energies overall and the most variation within each cluster, creating larger SEM than the other FGIN-1 compounds. Despite the differences in binding energies, FGIN-1-43 only varied in conformation from the other FGIN-1 compounds in conformation *b* because the chlorophenyl ring did not fit close to Tyr369. Of FGIN-1-43's 36 clusters non-background clusters, 40% were in conformation *c,* 29% in conformation *d* and the remaining 31% split between conformations *a* and *b*. Even with the higher binding energies, it is still theoretically possible for FGIN-1-43 to interact with 17 residues on helices 3, 5, 6, 7, and 10/11 in an energetically favorable fashion.

3.5.6. Docking of PK11195

The most well known TSPO ligand, PK11195, was also docked into the LBD of FXR. Since PK11195 only had 5 possible flexible torsions, fewer GA runs were required to reach optimal refinement. Out of 600 GA runs, ADT formed 9 conformational clusters for PK11195 with free energy of binding ranging from -9.94 kcal/mol to -8.81 kcal/mol. Of these 9 clusters, 8 contained fewer than the random number value of conformations (600/9 = 66.7) so they were considered background binding. The

largest cluster contained 496 conformations represented by an average binding energy of -9.64 ± 0.005 kcal/mol. Figure 11F shows that PK11195 adopted only one possible conformation within the pocket with no possibility or opportunity to form any hydrogen bonds, but was close enough to form hydrophobic interactions with 17 amino acids on helices 3, 5, 7, 10/11, and 12.

3.5.7. Mutational studies of FXR

Since the molecular modeling studies were based on a fixed crystal structure, as opposed to a fully flexible molecule in a biological environment, point mutations formed in FXR were necessary to validate the studies. Only CDCA and FGIN-1-27 were examined due to their capacity to hydrogen bond. (Though FGIN-1-20 was also able to form a hydrogen bond, this compound is not commercially available). Figure 12A shows the conformations of CDCA and FGIN-1-27 explained above. The docking studies demonstrated that these compounds formed hydrogen bonds with Thr288 (helix 3), Arg331 (helix 5), Tyr369 (helix 7) or His447 (helix 10/11), so single amino acid mutations of these residues were formed (Table 2). Ser332 is the only other residue in the pocket that could form hydrogen bonds with side chain atoms so a mutation was also created for this residue as another potential key residue. As a control, ZR-75-1 cells were evaluated with and without exogenous FXR to compare to changes caused by mutated residues. In each mutation, the basal activation of FXR was decreased compared to the wild-type FXR transfection. Both CDCA and FGIN-1-27 hydrogen bonded to T288 *in silico*; when threonine (T288L) was mutated, activation by CDCA decreased to basal while FGIN-1-27 decreased by about half.

Only CDCA in conformation *b* hydrogen bonded to R331, so as expected, the arginine mutation (R331L) prevented CDCA-induced expression, whereas FGIN-1-27 was not affected. Conformation *b* of FGIN-1-27 hydrogen bonded to tyrosine 369, but Y369L mutation resulted in a gain of function for FGIN-1-27. As expected, the Y369 mutation showed no change in CDCA. As predicted for CDCA in conformation *b*, the histidine mutation (H447F) prevented luciferase expression. The H447F mutation decreased activity also in response to FGIN-1-27. Even though no hydrogen bonding was seen with Ser332, the mutation (S332F) decreased luciferase activity also with both CDCA and FGIN-1-27 treatments.

4. DISCUSSION

FXR is involved in multiple aspects of the maintenance of bile acid homeostasis acting as a mediator between bile acid synthesis and efflux from the liver (8). The alternative pathway of bile acid synthesis requires TSPO for the translocation of cholesterol into the mitochondria (29). Since both FXR and TSPO are important for maintaining bile acid homeostasis, it is not improbable that a single compound modulates the activity of each of these proteins. We first looked at a GABA-ergic chemical library in order to identify chemical treatments, already known as TSPO ligands, that increase transcription of an FXR-regulated luciferase reporter. We identified one compound, FGIN-1-27, that activated FXR to a level similar to CDCA (Fig. 3A). FGIN-1-27 was one of the specific TSPO ligands in the F series of compounds in the chemical library; therefore, we chose two other structurally similar TSPO ligands (FGIN-1-43 and PK11195) to investigate further.

Our studies show that FGIN-1-27 is a partial agonist of FXR (Fig. 6). We show through *in vitro* luciferase reporter gene assays that treatment of FGIN-1-27 activates FXR-mediated transcription but decreases FXR activation by CDCA when CDCA concentration is not limiting (100 μM). Even though the FXR ligand-binding pocket preferentially binds amphipathic, non-planar bile acids that allow polar entities to form hydrogen bonds with amino acid residues (86), FGIN-1-27 fits into this pocket also. Based on the size of the pocket and of the individual molecules, it is unlikely that both CDCA and FGIN-1-27 bind to the pocket at the same time. According to *in silico*

molecular modeling results, FGIN-1-27 fits into the pocket with low binding energies, comparable to those of CDCA (Fig. 11A and 11B). Both CDCA and FGIN-1-27 hydrogen bond to the same amino acid (T288) *in silico*, and show no FXR-activation when H447 is mutated into phenylalanine (Fig. 12), which shows that both compounds bind similarly inside the pocket and compete for binding positions. Because CDCA has more atoms that can form hydrogen bonds, compared to FGIN-1-27, CDCA can fit into the binding pocket in more than one favorable position with more favorable agonist binding. This is evident when CDCA (100 μM) is treated with FGIN-1-27 (10 μM); FGIN-1-27 antagonizes the effects of CDCA. However, when FGIN-1-27 and CDCA are both at 10 μM, FGIN-1-27 binding is the main factor contributing to the increase in reporter gene transcription. Under normal circumstances, however, CDCA concentration would rarely reach 100 μM, as seen in a study of bile acid concentrations in the liver (87), where the average concentration of CDCA was 45 μM (30 nmol/g)[2]. Only with gallstone obstruction did the CDCA concentration reach 96 μM (64 nmol/g). Therefore, treatment with FGIN-1-27 *in vivo* would be predicted to show only agonist effects on FXR.

In this binding study, CDCA fits into the FXR ligand-binding pocket, with 87% of the possible conformations oriented so the C-24 carboxylate group hydrogen bonds with Thr288 (Fig. 11A and 12A). The 7α-hydroxyl group of CDCA in the remaining 13% of the conformations hydrogen bonds with H447 and the C-24 oxygen binds to Arg331. In accordance with modeling studies performed by other groups, CDCA

[2] This calculation was based on a 1.5 kg adult liver

orients itself similarly by positioning the 3α-hydroxyl group near His447, allowing the C-24 carboxylate group to hydrogen bond to Arg331 (86), or it is oriented so the C-24 carboxylate oxygens hydrogen bond to Leu348 (78). The results of this study position CDCA (conformation *a*) in an orientation more similar to that typically adopted by steroid hormones, and MFA-1, with the steroid rings rotated so that the 3α-hydroxyl group is near Arg331 (Fig. 11A).

It is possible that there is more than one functional orientation of CDCA in the LBD that can cause agonist ligand effects from hydrogen bonding to more than one residue. Our point mutation studies of FXR show that Thr288, Arg331 and His447 were the key residues responsible for the agonist effects of CDCA (Fig. 12B), all of which formed hydrogen bonds *in silico*. This suggests that the 7α-hydroxyl and C-24 oxygens are key attributes for CDCA. Our studies are in agreement with other studies that have shown the 3α-hydroxyl group, present on all bile acids, is not necessary for FXR activation (86) and an oxygen in either a carboxyl group or an alcohol on C-24 is responsible for the enhanced ligand potency (88). It is most likely a combination of the hydrophobicity of CDCA and available oxygens to form hydrogen bonds that confers agonist-binding properties, and allows CDCA to bind in more than one conformation.

Although the FXR ligand-binding pocket evolved to recognize non-planar amphipathic bile acids (86), FXR is able to bind compounds also with planar components, such as the FGIN-1 compounds. All four FGIN-1 compounds subjected to *in silico* modeling fit into four main conformations, *a, b, c* and *d* (Fig. 11B-11E).

Although the orientations within the pocket are similar, the ranges of binding energies vary among the FGIN-1 compounds. Since the FGIN-1 compounds have the same core structure, there may be no discrepancy in the initial recognition of the compound by FXR, however, once inside the pocket differences in binding occur. Removal of the fluorine from FGIN-1-27 (FGIN-1-51) did not inhibit binding inside the pocket of FXR (Fig. 11D). This suggests that the fluorine is not necessary for FGIN-1-27 to enter the pocket, but it could still be responsible for its agonist effects. The fluorine in FGIN-1-27 hydrogen bonded to Thr288 and Y369 *in silico,* however, mutational studies show that Tyr369 is not responsible agonist effects of ligand binding of FGIN-1-27 and Thr288 only decreased FXR-activity by about half. This discrepancy may be due to the dimensions of the crystallized pocket formed by MFA-1 (Fig. 10), not truly reflecting a biologically active flexible protein. The majority of the conformations of all these compounds docked fit into an "L" shape configuration with the bottom of the "L" pointing towards Thr288. The phenol group on MFA-1 most likely formed an additional crevice in the protein allowing ligands to bend when docked into the crystal structure, even though the 3BEJ structure closely resembled that of a rat receptor structure crystallized with 6-ethyl-CDCA (80). In a non-computerized environment where the entire protein can be flexible, this pocket may not form with all ligands. In a constantly flexible cellular environment, it is possible that the fluorine of FGIN-1-27 in conformation *c* could hydrogen bond to His447. This would correlate with the mutation of His447 diminishing FXR-activation by FGIN-1-27 (Fig. 12B). Upon entry into the pocket, it is conceivable that the FGIN-1 compounds would favor conformations *c* or *d* and never bend into an "L" shaped conformation. When Arg331

is mutated into leucine, little change is seen in FGIN-1-27 activity compared with wild-type FXR (Fig. 12B). If FGIN-1-27 was in conformation *d*, fluorine could conceivably hydrogen bond to the arginine, however, since Arg331 seems to have no significant interaction with FGIN-1-27, conformation *c* with the fluorophenyl group near His447 is more probable. Although the mutation of Ser332 (S332F) eliminates FXR-activation by treatments of both CDCA and FGIN-1-27, the addition of the bulky phenylalanine residue is most likely large enough to block the entrance to the binding pocket preventing any ligand entry.

To examine whether the hydrocarbon tails were factors in the binding of the FGIN-1 compounds, FGIN-1-20 was subjected to evaluation (Fig. 11C). The original study with the FGIN-1 compounds (72) found the binding affinity to TSPO increased with increasing alkyl chain lengths, up to 6 carbons. In this study, however, decreasing the number of carbons on the hydrophobic tails minimally changes the binding orientations in conformations *a* and *b,* with little difference in binding energies. However, the longer hydrophobic carbon tails in the other FGIN-1 compounds that fold alongside the indole backbone in conformations *c* and *d* create hydrophobic interactions favorable for ligand binding. The binding orientation changes when 3 carbons from each tail are removed; FGIN-1-20 does not fit into conformation *d.* Additionally, the oxygen on FGIN-1-20 in conformation *c* forms a hydrogen bond with His447. This orientation is unlikely to occur in structures with long hydrocarbon tails, such as FGIN-1-27, because the tails would cause steric hindrance. We did, however, see complete elimination of the agonist effects of FGIN-1-27 with the

H447F mutation of FXR, but this correlates with earlier speculations that the FGIN-1 compounds may favor conformation *c* upon entry into the pocket with fluorine of FGIN-1-27 hydrogen bonding to His447.

The addition of chlorine does not prevent FGIN-1-43 from fitting into the binding pocket of FXR; instead, it only forms unfavorable binding energies (Fig. 11E). For this compound, conformation *c* is favored most often. It is possible that the sheer size of chlorine prevents FGIN-1-43 from binding efficiently. Interestingly, FGIN-1-43 is better at antagonizing the agonist effects of FGIN-1-27 on FXR more so than with CDCA (Fig. 6). This suggests that FXR can recognize the core indole-acetamide structure without discrimination, but FGIN-1-27 has a higher binding affinity. When both FGIN-1 compounds are present, both will go into the pocket, but FGIN-1-27 will bind more favorably than FGIN-1-43. Similarly, because FGIN-1-43 does not bind to any residues specifically, CDCA will bind more efficiently so FGIN-1-43 will be displaced easier in the presence of CDCA. This idea also explains the antagonist effects of PK11195 on both CDCA and FGIN-1-27. According to the modeling results, PK11195 fits only into one orientation with an inhibition constant very similar to CDCA (Fig. 11F). Even though PK11195 does not interact with any residues specifically, it is oriented so access to His447 is blocked. When PK11195 is in the presence of an agonist ligand, PK11195 could compete for occupancy of the pocket of FXR and prevent CDCA or FGIN-1-27 from binding (Fig. 6).

In these studies, we had to take into account the possibility of the FGIN-1 compounds binding to TSPO on the mitochondria to indirectly increase the synthesis of CDCA, and in turn, activate FXR. In fact, FGIN-1-43 is found to be a more potent TSPO ligand than FGIN-1-27 (72). If there were any downstream effects present, FGIN-1-43 would show equal, if not more, activation of FXR than FGIN-1-27. In all of the results, FGIN-1-43 never activates FXR, thus demonstrating FXR activation by FGIN-1-27 is not a result of TSPO ligand binding.

We also show that FGIN-1-27 is as efficient as CDCA in recruiting the coactivator, SRC-1, to FXR LBD (Fig. 4). At 10 μM, FGIN-1-27 binding causes greater fold increase in luciferase expression than did CDCA treatment at 10 μM. The decrease in capability of PK11195 to recruit SRC-1 correlates with this compound being an antagonist. However, PK11195 does not antagonize BSEP and SHP expression as expected (Fig. 7 and 8). In fact, cotreatment of PK11195 with CDCA and FGIN-1-27 shows either little change or an increase in BSEP and SHP expression in HuH-7 cells and primary hepatocytes. Dussault et al (54) identified synthetic ligands of FXR that are gene-selective and modulate SHP and CYP7A1 expression differently. The discrepancy in PK11195 binding could be explained if the compound possesses different antagonistic effects based on the target gene. It is also likely that PK11195 binds to a number of different receptors. For example, in human hepatocytes, PK11195 is an agonist of pregnane x receptor (PXR; NR1I2) and an inverse agonist of constitutive androstane receptor (CAR; NR1I3), both also nuclear receptors (89), although HuH-7 cells do not express detectable levels of either PXR or CAR. In

HH1498, where SHP is not limiting, PK11195 treatment causes a significant increase in SHP mRNA expression, but PK11195 does not inhibit CYP7A1 expression at the same level as CDCA or FGIN-1-27 (Fig. 9). Our data shows PK11195 has little agonist effect on FXR alone, therefore, this increase in SHP expression and lack of full CYP7A1 repression could be due to PK11195 binding to LRH-1. If this were the case, PK11195 could prevent SHP from binding to LRH-1, thus eliminating the repressor function of SHP. Further studies of PK11195 binding to LRH-1 to cause direct transcriptional effects are necessary to validate this theory.

In these experiments, FGIN-1-27 proves to be at least equally as potent a ligand of FXR as CDCA at 10 μM, despite inevitable variations between individual hepatocyte cases. FGIN-1-27 increases both BSEP and SHP expression significantly, while repressing CYP7A1 expression, as expected (Fig. 7-9). FGIN-1-43 and PK11195 treatments, however, rarely cause any differences in gene expression from FXR activation. With all data considered, we conclude that FGIN-1-43 is a selective antagonist, competing only with the ligand with similar binding affinities to itself (FGIN-1-27) and PK11195 is a non-selective antagonist.

In addition to showing that these TSPO ligands modulate FXR, we also investigated a cell line with non-limiting endogenous FXR and RXR as an alternative to human hepatocytes (Fig. 5). Although primary human hepatocytes are the best *in vitro* representation of human liver, they vary among individuals and are expensive and difficult to acquire and maintain. Therefore, HuH-7 cells are beneficial for FXR

studies since they can be cultured in large numbers and passaged repeatedly. Unfortunately, HuH-7 lack SHP, so studies involving CYP7A1 repression through the SHP pathway may be difficult. Additionally, we show that the breast carcinoma cell line, ZR-75-1, has very little endogenous FXR with non-limiting endogenous RXR. Therefore, this cell line is ideal for mutational studies to avoid the interference of endogenous FXR.

In summary, targeting the rate-limiting step in the alternative pathway would be beneficial for upregulating this pathway. Correspondingly, TSPO ligands are known to increase cholesterol uptake into the mitochondria, which has been proven to be the rate-limiting step for the alternative pathway (29). Although controversial, some studies have shown that bile acids do not regulate CYP27A1 expression the same as CYP7A1 (68,69), which is not surprising since increasing CYP27A1 expression does not affect bile acid synthesis rates (29). Therefore, upregulating the alternative pathway apart from bile acid activation would be beneficial in people possessing faulty genes for CYP7A1 because the alternative pathway is heavily relied upon. However, in healthy populations an upregulation would not be necessary since the alternative pathway contributes little to the overall synthesis (23).

We have shown that FGIN-1-27 increases FXR transcriptional activity to increase BSEP and SHP expression. Also, FGIN-1-27 increases the rate of cholesterol entering the mitochondria by binding to TSPO (72). As demonstrated in Figure 13, targeting both TSPO and FXR with one compound would increase the bile acid synthesis rate of

the alternative pathway while regulating homeostasis in the liver by controlling the negative feedback through FXR. This would occur by 1) FGIN-1-27 binding to TSPO, facilitating the transport of cholesterol into the mitochondria where 2) CYP27A1 would initiate the production of CDCA. Furthermore, 3) FGIN-1-27 binds to FXR to 4) increase BSEP expression that would increase the efflux of bile from the liver. As bile acids are removed from the liver, the bile acid pool would decrease and trigger more synthesis of CDCA, thus lowering the cholesterol pool.

Future studies will be necessary to investigate the changes in the production of bile acid intermediates following FGIN-1-27 treatment. Multiple other genes involved in bile/lipid homeostasis are activated by FXR, including phospholipid transport protein, intestinal bile acid binding protein, and multidrug resistant protein 2 (MRP2) (84). The regulation of these genes by FGIN-1-27 should be investigated to further characterize FGIN-1-27 as a potential therapeutic drug. Similarly, the liver x receptor (LXR; NR1H3) increases expression of CYP7A1 from increased oxysterol production in the alternative pathway (90), thus regulating cell cholesterol concentrations. It would be necessary also to explore the transcriptional effects of FGIN-1-27 on LXR. Overall, a better understanding of the involvement of the mitochondria and FGIN-1-27 (and related compounds) in nuclear receptor signaling will lead to possible therapies for individuals with hindered bile acid synthesis.

5. REFERENCES

1. Russell, D. W. (2003) *Annu Rev Biochem* **72**, 137-174
2. Jones, P. H. (2001) *Am J Manag Care* **7**, S289-298
3. Tabas, I. (2002) *J Clin Invest* **110**, 583-590
4. Zollner, G., and Trauner, M. (2009) *Br J Pharmacol* **156**, 7-27
5. Pikuleva, I. A. (2006) *Drug Metab Dispos* **34**, 513-520
6. Chiang, J. Y. L. (2009) *Journal of Lipid Research*
7. Pikuleva, I. A. (2006) *Pharmacol Ther* **112**, 761-773
8. Chiang, J. Y. (2002) *Endocr Rev* **23**, 443-463
9. Luoma, P. V. (2008) *Eur J Clin Pharmacol* **64**, 841-850
10. Guengerich, F. P. (2001) *Chem Res Toxicol* **14**, 611-650
11. Guengerich, F. P. (2008) *Chem Res Toxicol* **21**, 70-83
12. Guengerich, F. P. (1992) *FASEB J* **6**, 745-748
13. Riddick, D. S., Lee, C., Bhathena, A., Timsit, Y. E., Cheng, P. Y., Morgan, E. T., Prough, R. A., Ripp, S. L., Miller, K. K., Jahan, A., and Chiang, J. Y. (2004) *Drug Metab Dispos* **32**, 367-375
14. Nebert, D. W., and Russell, D. W. (2002) *Lancet* **360**, 1155-1162
15. Shefer, S., Hauser, S., Bekersky, I., and Mosbach, E. H. (1970) *J Lipid Res* **11**, 404-411
16. Bjorkhem, I., Andersson, O., Diczfalusy, U., Sevastik, B., Xiu, R. J., Duan, C., and Lund, E. (1994) *Proc Natl Acad Sci U S A* **91**, 8592-8596

17. Reiss, A. B., Martin, K. O., Javitt, N. B., Martin, D. W., Grossi, E. A., and Galloway, A. C. (1994) *J Lipid Res* **35**, 1026-1030

18. Lund, E. G., Guileyardo, J. M., and Russell, D. W. (1999) *Proc Natl Acad Sci USA* **96**, 7238-7243

19. Ferdinandusse, S., and Houten, S. M. (2006) *Biochim Biophys Acta* **1763**, 1427-1440

20. Bjorkhem, I. (2006) *J Intern Med* **260**, 493-508

21. Pikuleva, I. A., Babiker, A., Waterman, M. R., and Bjorkhem, I. (1998) *J Biol Chem* **273**, 18153-18160

22. Beigneux, A., Hofmann, A. F., and Young, S. G. (2002) *J Clin Invest* **110**, 29-31

23. Pullinger, C. R., Eng, C., Salen, G., Shefer, S., Batta, A. K., Erickson, S. K., Verhagen, A., Rivera, C. R., Mulvihill, S. J., Malloy, M. J., and Kane, J. P. (2002) *J Clin Invest* **110**, 109-117

24. Wang, J., Freeman, D. J., Grundy, S. M., Levine, D. M., Guerra, R., and Cohen, J. C. (1998) *J Clin Invest* **101**, 1283-1291

25. Couture, P., Otvos, J. D., Cupples, L. A., Wilson, P. W., Schaefer, E. J., and Ordovas, J. M. (1999) *J Lipid Res* **40**, 1883-1889

26. Hofman, M. K., Groenendijk, M., Verkuijlen, P. J., Jonkers, I. J., Mohrschladt, M. F., Smelt, A. H., and Princen, H. M. (2004) *Eur J Hum Genet* **12**, 935-941

27. Dubrac, S., Lear, S. R., Ananthanarayanan, M., Balasubramaniyan, N., Bollineni, J., Shefer, S., Hyogo, H., Cohen, D. E., Blanche, P. J., Krauss, R.

M., Batta, A. K., Salen, G., Suchy, F. J., Maeda, N., and Erickson, S. K. (2005) *J Lipid Res* **46**, 76-85

28. Cali, J. J., Hsieh, C. L., Francke, U., and Russell, D. W. (1991) *J Biol Chem* **266**, 7779-7783

29. Pandak, W. M., Ren, S., Marques, D., Hall, E., Redford, K., Mallonee, D., Bohdan, P., Heuman, D., Gil, G., and Hylemon, P. (2002) *J Biol Chem* **277**, 48158-48164

30. Anholt, R. R., Pedersen, P. L., De Souza, E. B., and Snyder, S. H. (1986) *J Biol Chem* **261**, 576-583

31. Delavoie, F., Li, H., Hardwick, M., Robert, J. C., Giatzakis, C., Peranzi, G., Yao, Z. X., Maccario, J., Lacapere, J. J., and Papadopoulos, V. (2003) *Biochemistry* **42**, 4506-4519

32. Anholt, R. R., De Souza, E. B., Oster-Granite, M. L., and Snyder, S. H. (1985) *J Pharmacol Exp Ther* **233**, 517-526

33. Joseph-Liauzun, E., Delmas, P., Shire, D., and Ferrara, P. (1998) *J Biol Chem* **273**, 2146-2152

34. Hauet, T., Yao, Z. X., Bose, H. S., Wall, C. T., Han, Z., Li, W., Hales, D. B., Miller, W. L., Culty, M., and Papadopoulos, V. (2005) *Mol Endocrinol* **19**, 540-554

35. West, L. A., Horvat, R. D., Roess, D. A., Barisas, B. G., Juengel, J. L., and Niswender, G. D. (2001) *Endocrinology* **142**, 502-505

36. Arakane, F., Sugawara, T., Nishino, H., Liu, Z., Holt, J. A., Pain, D., Stocco, D. M., Miller, W. L., and Strauss, J. F., 3rd. (1996) *Proc Natl Acad Sci U S A* **93**, 13731-13736

37. Papadopoulos, V., and Brown, A. S. (1995) *J Steroid Biochem Mol Biol* **53**, 103-110

38. Li, H., and Papadopoulos, V. (1998) *Endocrinology* **139**, 4991-4997

39. Jamin, N., Neumann, J. M., Ostuni, M. A., Vu, T. K., Yao, Z. X., Murail, S., Robert, J. C., Giatzakis, C., Papadopoulos, V., and Lacapere, J. J. (2005) *Mol Endocrinol* **19**, 588-594

40. Tsankova, V., Visentin, M., Cantoni, L., Carelli, M., and Tacconi, M. T. (1996) *Eur J Pharmacol* **299**, 197-203

41. Stedman, C., Liddle, C., Coulter, S., Sonoda, J., Alvarez, J. G., Evans, R. M., and Downes, M. (2006) *Proc Natl Acad Sci U S A* **103**, 11323-11328

42. Mangelsdorf, D. J., Thummel, C., Beato, M., Herrlich, P., Schutz, G., Umesono, K., Blumberg, B., Kastner, P., Mark, M., Chambon, P., and Evans, R. M. (1995) *Cell* **83**, 835-839

43. Kumar, R., and Thompson, E. B. (1999) *Steroids* **64**, 310-319

44. Mangelsdorf, D. J., and Evans, R. M. (1995) *Cell* **83**, 841-850

45. Collingwood, T. N., Urnov, F. D., and Wolffe, A. P. (1999) *J Mol Endocrinol* **23**, 255-275

46. Wang, H., Chen, J., Hollister, K., Sowers, L. C., and Forman, B. M. (1999) *Mol Cell* **3**, 543-553

47. Forman, B. M., Goode, E., Chen, J., Oro, A. E., Bradley, D. J., Perlmann, T., Noonan, D. J., Burka, L. T., McMorris, T., Lamph, W. W., Evans, R. M., and Weinberger, C. (1995) *Cell* **81**, 687-693

48. Seol, W., Choi, H. S., and Moore, D. D. (1995) *Mol Endocrinol* **9**, 72-85

49. Sinal, C. J., Tohkin, M., Miyata, M., Ward, J. M., Lambert, G., and Gonzalez, F. J. (2000) *Cell* **102**, 731-744

50. Makishima, M., Okamoto, A. Y., Repa, J. J., Tu, H., Learned, R. M., Luk, A., Hull, M. V., Lustig, K. D., Mangelsdorf, D. J., and Shan, B. (1999) *Science* **284**, 1362-1365

51. Parks, D. J., Blanchard, S. G., Bledsoe, R. K., Chandra, G., Consler, T. G., Kliewer, S. A., Stimmel, J. B., Willson, T. M., Zavacki, A. M., Moore, D. D., and Lehmann, J. M. (1999) *Science* **284**, 1365-1368

52. Maloney, P. R., Parks, D. J., Haffner, C. D., Fivush, A. M., Chandra, G., Plunket, K. D., Creech, K. L., Moore, L. B., Wilson, J. G., Lewis, M. C., Jones, S. A., and Willson, T. M. (2000) *J Med Chem* **43**, 2971-2974

53. Downes, M., Verdecia, M. A., Roecker, A. J., Hughes, R., Hogenesch, J. B., Kast-Woelbern, H. R., Bowman, M. E., Ferrer, J. L., Anisfeld, A. M., Edwards, P. A., Rosenfeld, J. M., Alvarez, J. G., Noel, J. P., Nicolaou, K. C., and Evans, R. M. (2003) *Mol Cell* **11**, 1079-1092

54. Dussault, I., Beard, R., Lin, M., Hollister, K., Chen, J., Xiao, J. H., Chandraratna, R., and Forman, B. M. (2003) *J Biol Chem* **278**, 7027-7033

55. Urizar, N. L., Liverman, A. B., Dodds, D. T., Silva, F. V., Ordentlich, P., Yan, Y., Gonzalez, F. J., Heyman, R. A., Mangelsdorf, D. J., and Moore, D. D. (2002) *Science* **296**, 1703-1706

56. Goodwin, B., Jones, S. A., Price, R. R., Watson, M. A., McKee, D. D., Moore, L. B., Galardi, C., Wilson, J. G., Lewis, M. C., Roth, M. E., Maloney, P. R., Willson, T. M., and Kliewer, S. A. (2000) *Mol Cell* **6**, 517-526

57. Lu, T. T., Makishima, M., Repa, J. J., Schoonjans, K., Kerr, T. A., Auwerx, J., and Mangelsdorf, D. J. (2000) *Mol Cell* **6**, 507-515

58. Lee, Y. K., and Moore, D. D. (2002) *J Biol Chem* **277**, 2463-2467

59. Chen, W., Owsley, E., Yang, Y., Stroup, D., and Chiang, J. Y. (2001) *J Lipid Res* **42**, 1402-1412

60. Lee, Y. K., Dell, H., Dowhan, D. H., Hadzopoulou-Cladaras, M., and Moore, D. D. (2000) *Mol Cell Biol* **20**, 187-195

61. Sanyal, S., Bavner, A., Haroniti, A., Nilsson, L. M., Lundasen, T., Rehnmark, S., Witt, M. R., Einarsson, C., Talianidis, I., Gustafsson, J. A., and Treuter, E. (2007) *Proc Natl Acad Sci U S A* **104**, 15665-15670

62. Nitta, M., Ku, S., Brown, C., Okamoto, A. Y., and Shan, B. (1999) *Proc Natl Acad Sci U S A* **96**, 6660-6665

63. Crestani, M., Sadeghpour, A., Stroup, D., Galli, G., and Chiang, J. Y. (1998) *J Lipid Res* **39**, 2192-2200

64. Ananthanarayanan, M., Balasubramanian, N., Makishima, M., Mangelsdorf, D. J., and Suchy, F. J. (2001) *J Biol Chem* **276**, 28857-28865

65. Plass, J. R., Mol, O., Heegsma, J., Geuken, M., Faber, K. N., Jansen, P. L., and Muller, M. (2002) *Hepatology* **35**, 589-596

66. Gerloff, T., Stieger, B., Hagenbuch, B., Madon, J., Landmann, L., Roth, J., Hofmann, A. F., and Meier, P. J. (1998) *J Biol Chem* **273**, 10046-10050

67. Repa, J. J., Turley, S. D., Lobaccaro, J. A., Medina, J., Li, L., Lustig, K., Shan, B., Heyman, R. A., Dietschy, J. M., and Mangelsdorf, D. J. (2000) *Science* **289**, 1524-1529

68. Bjorkhem, I., Araya, Z., Rudling, M., Angelin, B., Einarsson, C., and Wikvall, K. (2002) *J Biol Chem* **277**, 26804-26807

69. Abrahamsson, A., Gustafsson, U., Ellis, E., Nilsson, L. M., Sahlin, S., Bjorkhem, I., and Einarsson, C. (2005) *Biochem Biophys Res Commun* **330**, 395-399

70. Casellas, P., Galiegue, S., and Basile, A. S. (2002) *Neurochem Int* **40**, 475-486

71. Le Fur, G., Perrier, M. L., Vaucher, N., Imbault, F., Flamier, A., Benavides, J., Uzan, A., Renault, C., Dubroeucq, M. C., and Gueremy, C. (1983) *Life Sci* **32**, 1839-1847

72. Romeo, E., Auta, J., Kozikowski, A. P., Ma, D., Papadopoulos, V., Puia, G., Costa, E., and Guidotti, A. (1992) *J Pharmacol Exp Ther* **262**, 971-978

73. Romeo, E., Cavallaro, S., Korneyev, A., Kozikowski, A. P., Ma, D., Polo, A., Costa, E., and Guidotti, A. (1993) *J Pharmacol Exp Ther* **267**, 462-471

74. Korneyev, A., Pan, B. S., Polo, A., Romeo, E., Guidotti, A., and Costa, E. (1993) *J Neurochem* **61**, 1515-1524

75. Laffitte, B. A., Kast, H. R., Nguyen, C. M., Zavacki, A. M., Moore, D. D., and Edwards, P. A. (2000) *J Biol Chem* **275**, 10638-10647

76. Auerbach, S. S., Stoner, M. A., Su, S., and Omiecinski, C. J. (2005) *Mol Pharmacol* **68**, 1239-1253

77. Omiecinski, C. J., Redlich, C. A., and Costa, P. (1990) *Cancer Res* **50**, 4315-4321

78. Kaimal, R., Song, X., Yan, B., King, R., and Deng, R. (2009) *J Pharmacol Exp Ther*

79. Song, X., Kaimal, R., Yan, B., and Deng, R. (2008) *J Lipid Res* **49**, 973-984

80. Soisson, S. M., Parthasarathy, G., Adams, A. D., Sahoo, S., Sitlani, A., Sparrow, C., Cui, J., and Becker, J. W. (2008) *Proc Natl Acad Sci U S A* **105**, 5337-5342

81. Morris, G. M. G., David S.; Pique, Michael E.; Lindstrom, William; Huey, Ruth; Forli, Stefano; Hart, William E.; Halliday, Scott; Belew, Rik; Olson, Arthur J. (2010) AutoDock Version 4.2: Automated Docking of Flexible Ligands to Flexible Receptors.

82. Evans, R. M. (2005) *Mol Endocrinol* **19**, 1429-1438

83. Bramlett, K. S., Yao, S., and Burris, T. P. (2000) *Mol Genet Metab* **71**, 609-615

84. Lee, F. Y., Lee, H., Hubbert, M. L., Edwards, P. A., and Zhang, Y. (2006) *Trends Biochem Sci* **31**, 572-580

85. Carosati, E., Sciabola, S., and Cruciani, G. (2004) *J Med Chem* **47**, 5114-5125

86. Mi, L. Z., Devarakonda, S., Harp, J. M., Han, Q., Pellicciari, R., Willson, T. M., Khorasanizadeh, S., and Rastinejad, F. (2003) *Mol Cell* **11**, 1093-1100

87. Honda, A., Yoshida, T., Tanaka, N., Matsuzaki, Y., He, B., Shoda, J., and Osuga, T. (1995) *J Gastroenterol* **30**, 61-66

88. Fujino, T., Une, M., Imanaka, T., Inoue, K., and Nishimaki-Mogami, T. (2004) *J Lipid Res* **45**, 132-138

89. Li, L., Chen, T., Stanton, J. D., Sueyoshi, T., Negishi, M., and Wang, H. (2008) *Mol Pharmacol* **74**, 443-453

90. Chawla, A., Repa, J. J., Evans, R. M., and Mangelsdorf, D. J. (2001) *Science* **294**, 1866-1870

91. Papadopoulos, V., Baraldi, M., Guilarte, T. R., Knudsen, T. B., Lacapere, J. J., Lindemann, P., Norenberg, M. D., Nutt, D., Weizman, A., Zhang, M. R., and Gavish, M. (2006) *Trends Pharmacol Sci* **27**, 402-409

6. ABBREVIATIONS

ADT: AutoDock tools

AF-2: activation function-2 domain

BSEP: bile salt export pump

CA: cholic acid

CDCA: chenodeoxycholic acid

COS-1: African Green Monkey kidney cell line transformed with Simian Virus 40

CTX: cerebrotendinous xanthomatosis

CYP7A1: cholesterol 7α-hydroxylase

CYP7B1: 25-hydroxycholesterol 7α-hydroxylase

CYP8B1: sterol 12α-hydroxylase

CYP27A1: sterol 27-hydroxylase

CYP39A1: oxysterol 7α-hydroxylase

CYP46A1: cholesterol 24α-hydroxylase

DMEM: Dulbecco's Modified Eagle Medium

DMSO: dimethyl sulfoxide

DR: direct repeat

ER: everted repeat

FBS: fetal bovine serum

FGIN-1: 2-aryl-3-acetamide compounds from Fidia-Georgetown Institute for the Neuorsciences (72)

FGIN-1-20: N, N-di-n-propyl 2-(4-fluorophenyl) indole-3-acetamide

FGIN-1-27: N, N-di-n-hexyl 2-(4-fluorophenyl) indole-3-acetamide

FGIN-1-43: N, N-dihexyl 2-(4-chlorophenyl) 5-chloroindole-3-acetamide

FGIN-1-51: N, N-di-n-hexyl 2-(4-phenyl) indole-3-acetamide

FXR: farnesoid x receptor

FXRE: FXR response element

GA: genetic alorithm

GABA: γ-aminobutryic acid

HH1486: human hepatocyte case #1486

HH1498: human hepatocyte case #1498

HMG-CoA: 3-hydroxy-3methylglutaryl-coenzyme A

HNF4: hepatic nuclear factor-4

HuH-7: human hepatoma cell line

IR: inverted repeat

LDL-C: low-density lipoprotein cholesterol

LBD: ligand binding domain

LRH-1: liver receptor homolog-1

MFA-1: Merck FXR agonist #1 (17β-(4-hydroxybenzoyl) androsta-3, 5-diene-3-carboxylic acid)

OMM: outer mitochondrial membrane

PK11195: 1-(2-chlorophenyl)-N-methyl-N-(1-methylprolyl)-3-isoquinoline carboxamide

PDB: protein data bank

RMS: root-mean-square

RXRα: retinoid x receptor

SHP: small heterodimer partner

SRC-1: steroid receptor coactivator-1

STAR: steroidogenic acute regulatory protein

TK: thymidine kinase

TSPO: translocator protein (18 kDa), formerly known as peripheral-type benzodiazepine receptor (PBR) (91)

UAS: upstream activation sequence

ZR-75-1: breast cancer cell line

7. FIGURE LEGENDS

Figure 1: **CYP enzymes involved in the two pathways of bile acid synthesis.** CYP7A1 initiates the classic/neutral pathway to produce cholic acid (CA) and chenodeoxycholic acid (CDCA). CYP27A1 and CYP46A1 initiate alternative/acidic pathway forming oxysterols that must undergo 7α-hydroxylation before becoming CDCA. The carbons on cholesterol are numbered to correspond with the names of each intermediate formed by each CYP enzyme shown (boxed); changes to each structure are illustrated in red. Note: other non-CYP enzymes are also involved in these pathways.

Figure 2: **The role of STAR and TSPO in cholesterol transport into the mitochondria.** Intracellular cholesterol binds to STAR, and through a complex pathway involving other proteins not shown, cholesterol is transported to the OMM. Cholesterol is then transferred to TSPO where ligand binding facilitates cholesterol uptake into the IMM where CYP27A1 resides. Cholesterol transport is the rate-limiting step in the alternative pathway for bile acid synthesis. CDCA will then be synthesized once in the liver.

Figure 3: **GABA-ergic chemical library screen of compounds and structures of CDCA, FGIN-1 compounds, and PK11195. A)** HuH-7 cells were transfected with 5 μg p(FXRE)$_4$-TK-luc and 0.5 μg pRL-CMV and treated for 24h with GABA-ergic compounds. Series B-F are single well 10 μM treatments with values reported as fold change relative to DMSO (control) (n=4). CDCA (n=4) is also 10 μM. F2 is FGIN-1-27, F3 is FGIN-1-43 and F10 is PK11195. **B)** Chemical structures of compounds mentioned in **A**. FGIN-1-27 has six carbons on R_3 with fluorine at R_1 and hydrogen at R_2. FGIN-1-43 has six carbons on R_3 with chlorine at R_1 and R_2.

Figure 4: **Coactivator recruitment to FXR in mammalian two-hybrid assay.** COS-1 cells were transfected with 5 μg of pFR-luc, 1.5 μg pM-SRC-1, 1.5 μg VP16-FXR and 0.5 μg pRL-CMV and treated for 24h. Luciferase activity of each treatment is reported as fold change relative to DMSO (control) represented by a solid line at 1.
* denotes significance compared to control, $p \leq 0.05$, (n=8).

Figure 5: **Cell line comparison of mRNA expression for proteins involved in FXR-mediated bile acid homeostasis. A)** Expression of FXR and RXR mRNA in human hepatocytes, HuH-7, and ZR-75-1 cell lines. Total RNA was reverse transcribed and cDNA was subjected to actin and select gene-specific amplification with SYBR green PCR. Gene expression was normalized to actin and expressed as fold relative to HH1498 mRNA expression (control) (n=2). **B)** mRNA expression of nuclear receptors involved in SHP-mediated regulation of bile acids (SHP, LRH-1, and HNF4α) in HH1498 and HuH-7. Gene expression was normalized to actin and expressed as fold relative to HH1498 (control) (n=2). **C)** HuH-7 cells and **D)** ZR-75-1 cells were transfected with 5 μg p(FXRE)$_4$-TK-luc, 0.5 μg pRL-CMV, and 1.25 μg of 3.1-FXR or pcDNA3.1(+) empty vector. Luciferase activity for treatments is shown relative to DMSO (control) (n=4).

* denotes significance compared to control, $p \leq 0.05$; † denotes significance compared to respective treatment in transfection with no exogenous FXR, $p \leq 0.05$.

Figure 6: **Effects of dose response cotreatments of CDCA with TSPO ligands on FXR-luciferase reporter activity.** HuH-7 cells were transfected with 5 μg $p(FXRE)_4$-TK-luc and 0.5 μg pRL-CMV and treated for 24h with CDCA, FGIN-1-27, FGIN-1-43 or PK11195 at varying concentrations. CDCA and FGIN-1-27 were cotreated with FGIN-1-43 and PK11195 at 10 μM and 1 μM concentrations. CDCA was also cotreated with FGIN-1-27 at 10 μM and 1 μM concentrations. All values (n=4) are expressed as fold relative to DMSO (control) (n=16). CDCA at 10 μM and 100 μM, n=8. White and dark grey bars represent cotreatments at 10 μM and 1 μM, respectively, with CDCA or FGIN-1-27 held constant at the noted concentration. * denotes significance compared to control, $p \leq 0.05$, represented by solid line. † denotes significance compared to respective constant treatment, represented by dotted line, $p \leq 0.05$.

Figure 7: **Expression of BSEP mRNA in response to ligands of FXR and TSPO.** Human hepatocytes (HH1486 and HH1498) and HuH-7 cells were treated for 24h at a final concentration of 10 μM. Total RNA was reverse transcribed and cDNA was subjected to actin and BSEP gene-specific amplification with SYBR green PCR. BSEP expression was normalized to actin and treatments are relative to DMSO (control) in each experiment. In HH1498 and HuH-7, CDCA and FGIN-1-27 were cotreated with FGIN-1-43 or PK11195. The CDCA and FGIN-1-27 control treatment values are represented by dotted lines. * denotes significance compared to control, $p \leq 0.05$. † denotes significance compared to respective constant treatment, represented by dotted line, $p \leq 0.05$, HH1486 (n=3), HH1498 (n=3), and HuH-7 (n=2).

Figure 8: **Expression of SHP mRNA in response to ligands of FXR and TSPO.** Human hepatocytes (HH1486 and HH1498) and HuH-7 cells were treated for 24h at a final concentration of 10 μM. Total RNA was reverse transcribed and cDNA was subjected to actin and SHP gene-specific amplification with SYBR green PCR. SHP expression was normalized to actin and treatments are relative to DMSO (control) in each experiment. In HH1498 and HuH-7, CDCA and FGIN-1-27 were cotreated with FGIN-1-43 or PK11195. The CDCA and FGIN-1-27 control treatment values are represented by dotted lines. * denotes significance compared to control, $p \leq 0.05$. † denotes significance compared to respective constant treatment, represented by dotted line, $p \leq 0.05$, HH1486 (n=3), HH1498 (n=3), and HuH-7 (n=2).

Figure 9: **Expression of CYP7A1 mRNA in human hepatocytes.** Human hepatocytes (HH1486 and HH1498) were treated for 24h at a final concentration of 10 μM. Total RNA was reverse transcribed and cDNA was subjected to actin and CYP7A1 gene-specific amplification with SYBR green PCR. CYP7A1 expression was normalized to actin and treatments are relative to DMSO (control) in each experiment. The schematic illustrates the direct repression of CYP7A1 gene expression by SHP via indirect FXR ligand activation. * denotes significance compared to control, $p \leq 0.05$, (n=3).

Figure 10: **Crystallized structure of FXR LBD with MFA-1 in the binding pocket (PDB ID code 3BEJ).** Each α-helix in the LBD is labeled (1-12) and varies by color for simpler visual representation. The small fragment of SRC-1 is shown in green.

Figure 11: **Molecular modeling of CDCA and TSPO ligands in the LBD of FXR.** Each compound formed various conformations, grouped into clusters, based upon orientation of each atom deviating by 2.0 Å RMS. On the graphs, each bar represents the number of conformations in a cluster with shared mean free energy of binding ± SEM. The brackets, labeled *a-d*, represent the binding energy range for each conformation based upon core ring orientation. Within each bracket, the hydrocarbon tails vary in position while the rings maintain the same conformation. The lowest energy conformers representing the four bracketed conformation types are shown with key amino acid residues highlighted: T = Thr288, R = Arg331, Y = Tyr369, and H = His447. Dotted black lines represent hydrogen bonds. Each table shows the frequency and mean free energy of binding ± SEM for each bracketed conformation. **A)** CDCA fit into two conformations from 600 GA runs forming hydrogen bonds with T288 in conformation *a* and with R331 and H447 in conformation *b*. **B)** FGIN-1-27 formed four main conformations from 800 GA runs forming hydrogen bonds with T288 in conformation *a* and with Y369 in conformation *b*. **C)** FGIN-1-20 fit into three conformations from 800 GA runs forming hydrogen bonds with T288 in conformation *a* and H447 in conformation *c*. **D)** Four conformations of FGIN-1-51 were formed from 800 GA runs. **E)** FGIN-1-43 found four conformations from 800 GA runs. **F)** Only one conformation resulted for PK11195 from 600 GA runs.

Figure 12: **Effects of point mutations of amino acids predicted to interact with ligands inside the LBD of FXR. A)** Two conformations (*a* and *b*) of CDCA and four conformations of FGIN-1-27 (*a-d*) with the lowest free energy of binding in the LBD of FXR. Hydrogen bonds to Thr288, Tyr369, His447 and Arg331 are represented by dotted black line. Residues that directly interact with the ligands are highlighted in yellow. **B)** ZR-75-1 cells were transfected with 1 μg of $p(FXRE)_4$-TK-luc, 100 ng pRL-CMV, and 500 ng of FXR, either wild type (WT) or hFXR mutant and treated for 24h with a final concentration of 10 μM. * denotes significance compared to control for each mutation, $p \leq 0.05$. (n=4). † denotes significance compared to respective treatment of WT FXR, $p \leq 0.05$.

Figure 13: **Involvement of FGIN-1-27 in the alternative pathways of bile acid synthesis and homeostasis.** 1) FGIN-1-27 binding to TSPO facilitates the transport of cholesterol into the mitochondria. 2) The alternative pathway of bile acid synthesis produces CDCA. 3) CDCA and FGIN-1-27 can both activate FXR to 4) increase BSEP gene expression.

8. TABLES

Table 1. *GABA-ergic chemical library*

NUMBER	COMPOUND	GABAergic ACTIVITY
B1	GABA	Endogenous ligand.
B2	3-Methyl-GABA	Activator of GABA aminotransferase.
B3	Gabaculine	Irreversible inhibitor of GABA transaminase.
B4	trans-4-Aminocrotonic acid	GABA agonist.
B5	cis-4-Aminocrotonic acid	GABAc receptor ligand.
B6	4,5,6,7-Tetrahydroisoxazolo[5,4-C]pyridin-3-ol	GABAa receptor agonist.
B7	(1,2,5,6-Tetrahydropyridin-4-yl)methylphosphinic acid	GABAc receptor antagonist.
B8	CGP 35348	GABAb antagonist.
B9	CGP 46381	GABAb antagonist.
B10	CGP 52432	GABAb antagonist.
B11	CGP 54626 HCl	GABAb antagonist.
B12	CGP 55845	GABAb antagonist.
C1	Saclofen hCl	Antagonist at GABAb receptors.
C2	SCH 50911	GABAb antagonist.
C3	Imidazole-4-acetic acid HCl	Partial GABAc agonist.
C4	Riluzole HCl	GABA uptake inhibitor.
C5	SKF 89976A HCl	GABA uptake inhibitor.
C6	Vigabatrin	GABA-T inhibitor.
C7	Propofol	GABAa agonist.
C8	Methyl-6,7-dimethoxy-4-ethyl-b-carboline-3-carboxylate	Benzodiazepine receptor inverse agonist
C9	(±)-4-Amino-3-(5-chloro-2-thienyl)-butanoic acid	GABAb agonist.
C10	(±)-Baclofen	GABAb agonist.
C11	(-)-Bicuculline methobromide	GABAa antagonist.
C12	Guvacine HCl	GABA uptake inhibitor.
D1	Isoguvacine HCl	GABA agonist.
D2	Muscimol	GABAa receptor agonist.
D3	Baclofen	GABAb receptor antagonist.
D4	SK&F 97541	GABAb agonist.
D5	ZAPA H2SO4	Agonist at low affinity GABAa receptors.
D6	Gabazine	Specific GABAa receptor antagonist.

NUMBER	COMPOUND	GABAergic ACTIVITY
D7	Chlormethiazole HCl	N/A
D8	Primidone	N/A
D9	Quisqualamine	GABAa receptor ligand.
D10	NCS-382	Antagonist of GHB.
D11	(1S,9R)-b-Hydrastine	GABAa receptor antagonist.
D12	Picrotoxinin	GABAa antagonist.
E1	5-a-Pregnan-3-a-ol-20-one	Positive allosteric modulator of GABAa Cl channel.
E2	5-a-Pregnane-3-a-2,1-diol-20-one	Positive allosteric modulator of GABAa receptors.
E3	Dimethyl Sulfoxide	Control
E4	Pentylenetetrazole	N/A
E5	trans-4-Hydroxycrotonic acid	GHB receptor ligand.
E6	NO-711 HCl	GABA uptake inhibitor.
E7	1-Amino-5-bromouracil	Benzodiazepine / GABAa ligand
E8	Methyl-b-carboline-3-carboxylate	Benzodiazepine inverse agonist.
E9	Butyl-b-carboline-3-carboxylate	Endogenous proconvulsant and anxiogenic benzodiazepine receptor ligand.
E10	Propyl-b-carboline-3-carboxylate	Benzodiazepine inverse agonist.
E11	Ethyl-b-carboline-3-carboxylate	Benzodiazepine inverse agonist.
E12	Chlormezanone	N/A
F1	7-(Dimethylcarbamoyloxy)-6-phenylpyrrolo-[2,1-D][1,5]benzothiazepine	Peripheral benzodiazepine receptor ligand
F2	FGIN-1-27	Peripheral benzodiazepine receptor ligand
F3	FGIN-1-43	Peripheral benzodiazepine receptor ligand
F4	GBLD 345	A high affinity benzodiazepine agonist.
F5	N-[-(4-Methoxyphenyl)ethyl]-3-indoleglyoxamide	An inverse agonist at the benzodiazepine receptor.
F6	FG 7142	Inverse agonist and anxiogenic agent.
F7	Zopiclone	A non benzodiazepine BZR agonist.
F8	Flumazenil	Benzodiazepine antagonist.
F9	3-Hydroxymethyl-b-carboline	Benzodiazepine inverse agonist.
F10	PK-11195	Peripheral benzodiazepine receptor ligand
F11	Isoniazid	Negative allosteric modulator of GABAa receptors.
F12	Isonicotinic acid	GABA receptor ligand.

Table 2. *Point mutations of FXR amino acids*

		Sequence (5' - 3')										
T288L	**AA Num.**	283	284	285	286	287	288	289	290	291	292	293
	Codon	aat	ttt	ctc	att	ttg	acg	gaa	atg	gca	acc	aat
	AA	N	F	L	I	L	T	E	M	A	T	N
	Codon Mutation	aat	ttt	ctc	att	ttg	ctg	gaa	atg	gca	acc	aat
	AA Mutation	N	F	L	I	L	L	E	M	A	T	N
R331L	**AA Num.**	326	327	328	329	330	331	332	333	334	335	336
	Codon	gaa	gct	atg	ttc	ctt	cgt	tca	gct	gag	att	ttc
	AA	E	A	M	F	L	R	S	A	E	I	F
	Codon Mutation	gaa	gct	atg	ttc	ctt	ctt	tca	gct	gag	att	ttc
	AA Mutation	E	A	M	F	L	L	S	A	E	I	F
S332F	**AA Num.**	327	328	329	330	331	332	333	334	335	336	337
	Codon	gct	atg	ttc	ctt	cgt	tca	gct	gag	att	ttc	aat
	AA	A	M	F	L	R	S	A	E	I	F	N
	Codon Mutation	gct	atg	ttc	ctt	cgt	ttt	gct	gag	att	ttc	aat
	AA Mutation	A	M	F	L	R	F	A	E	I	F	N
Y369L	**AA Num.**	364	365	366	367	368	369	370	371	372	373	374
	Codon	cct	atg	ttt	agt	ttt	tat	aaa	agt	att	ggg	gaa
	AA	P	M	F	S	F	Y	K	S	I	G	E
	Codon Mutation	cct	atg	ttt	agt	ttt	ctt	aaa	agt	att	ggg	gaa
	AA Mutation	P	M	F	S	F	L	K	S	I	G	E
H447F	**AA Num.**	442	443	444	445	446	447	448	449	450	451	452
	Codon	aca	ttc	aat	cat	cac	cac	gct	gag	atg	ctg	atg
	AA	T	F	N	H	H	H	A	E	M	L	M
	Codon Mutation	aca	ttc	aat	cat	cac	ttc	gct	gag	atg	ctg	atg
	AA Mutation	T	F	N	H	H	F	A	E	M	L	M

Table 3. *Forward and reverse oglionucleotide primer sequences for DNA amplification via SYBR Green RT-PCR*

	5'-3' Sequence
[redacted]in	F - GTTGTCGACGACGAGCG
	R - GCACAGAGCCTCGCCTT
[redacted]SEP	F - CATTTCGCTCTCGATGTTCA
	R - TTCCAGGAAAAGCATGTGTG
[redacted]YP7A1	F - GGTGCAAAGTGAAATCCTCC
	R - CAGAACTGAATGACCTGCCA
FXR	F - CACAGCGTTTTTGGTAATGC
	R - TTGTTTGTGGAGACAGAGCCT
[redacted]NF4	F - GGCTGCTGTCCTCATAGCTT
	R - GCAGGCTCAAGAAATGCTTC
[redacted]RH-1	F - CGGTAAATGTGGTCGAGGAT
	R - CGAGTGGGCCAGGAGTAGTA
RXRα	F - TGTCAATCAGGCAGTCCTTG
	R - GGGTGTACAGCTGCGAGGG
[redacted]HP	F - ACTTCACACAGCACCCAGT
	R - AGGGACCATCCTCTTCAACC

9. FIGURES

Figure 1

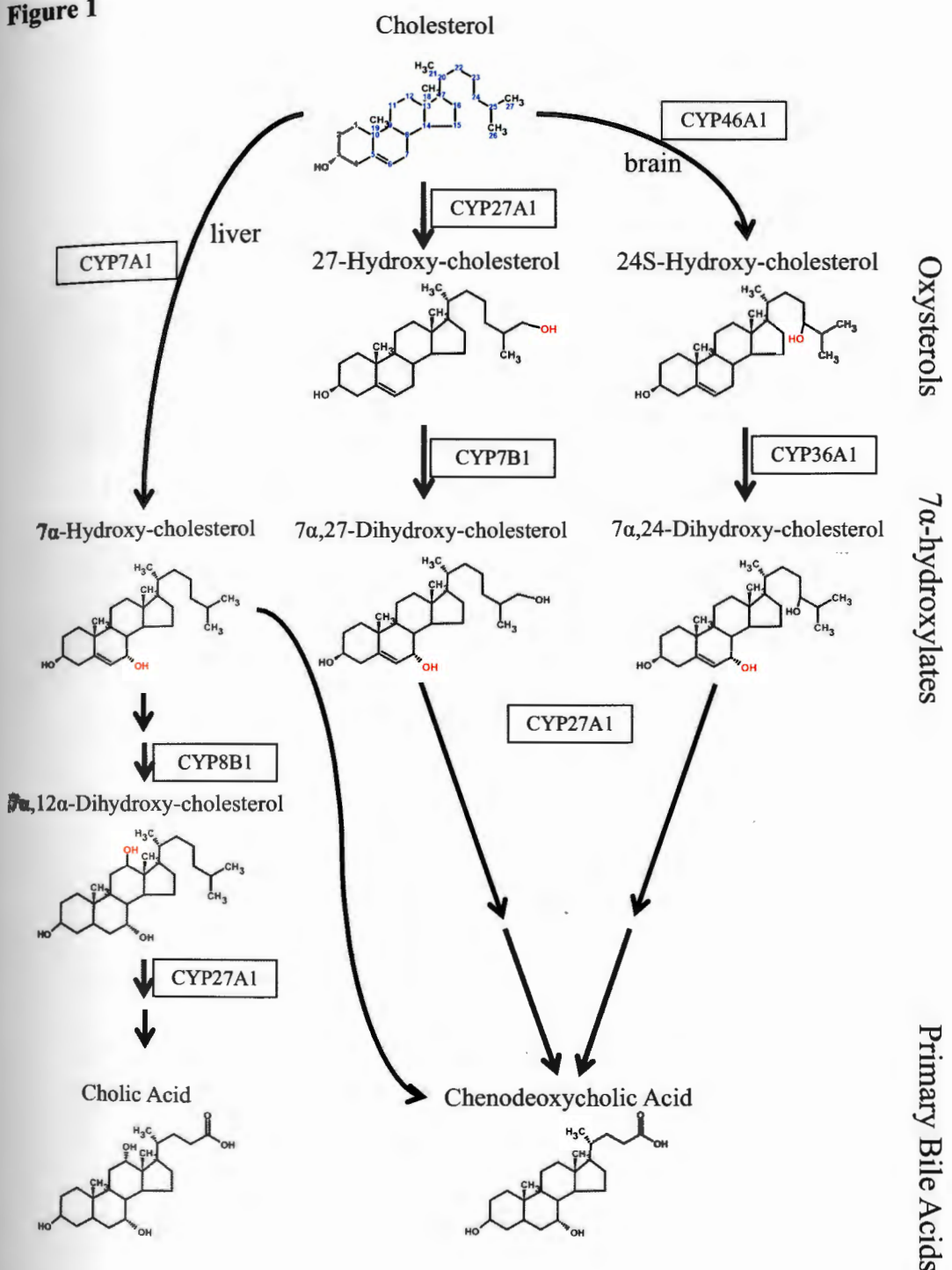

Figure 2

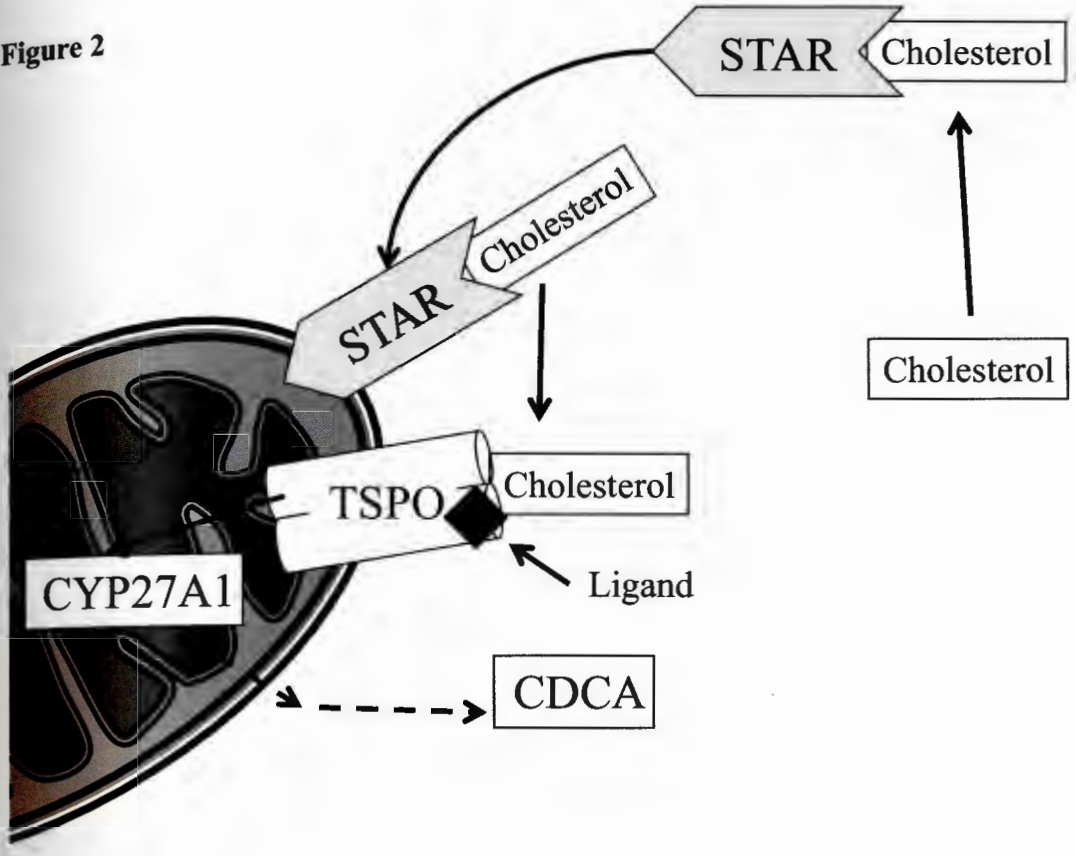
STAR
Cholesterol
Cholesterol
STAR
Cholesterol
TSPO
Cholesterol
Ligand
CYP27A1
CDCA

Figure 3

A

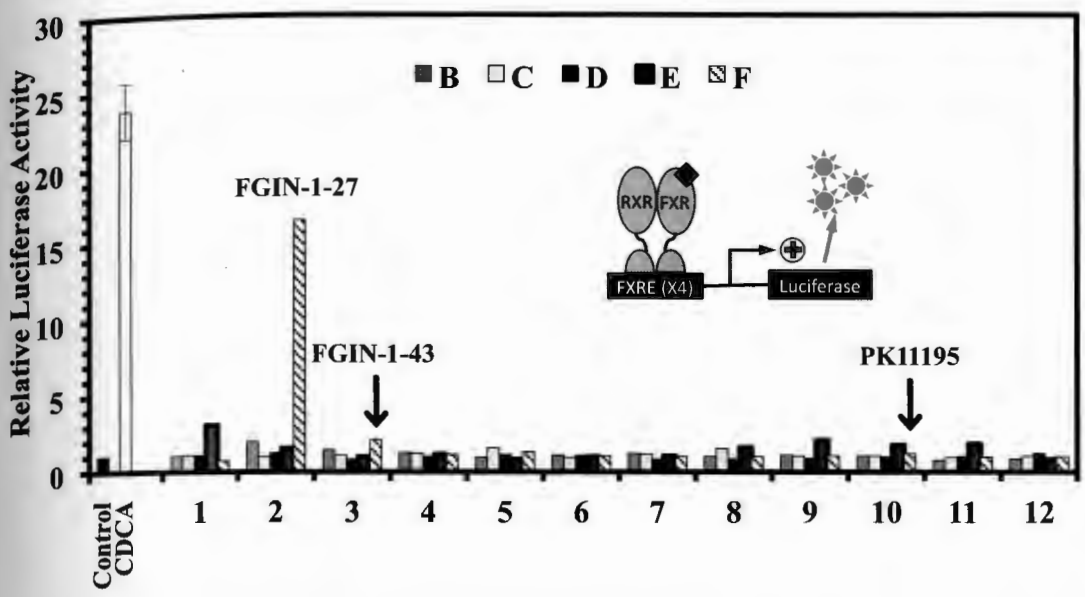

B

CDCA

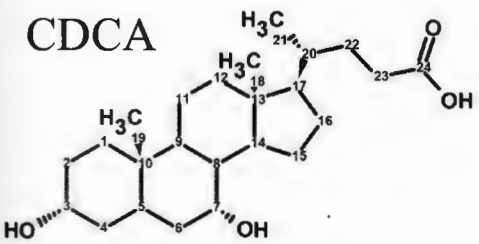

FGIN-1

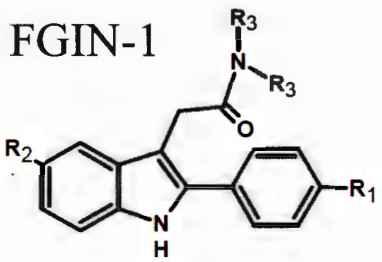

PK11195

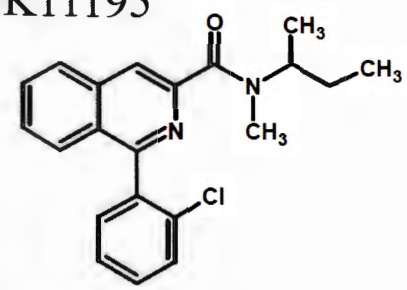

FGIN-1	R_1	R_2	R_3
27	F	H	Hexyl
43	Cl	Cl	Hexyl
20	F	H	Propyl
51	H	H	Hexyl

Figure 4

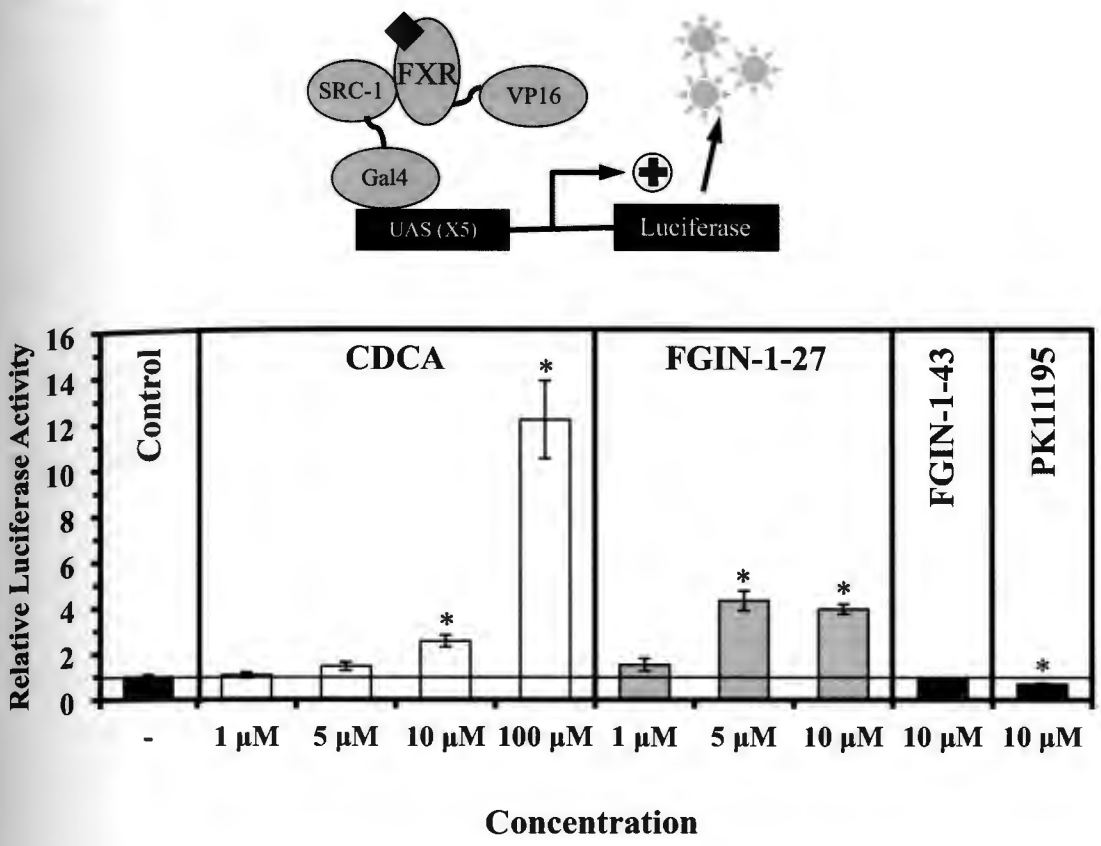
SRC-1
FXR
VP16
Gal4
UAS (X5)
Luciferase
Relative Luciferase Activity
16
14
12
10
8
6
4
2
0
Control
CDCA
FGIN-1-27
FGIN-1-43
PK11195
*
-
1 µM
5 µM
10 µM
100 µM
1 µM
5 µM
10 µM
10 µM
10 µM
Concentration

Figure 5

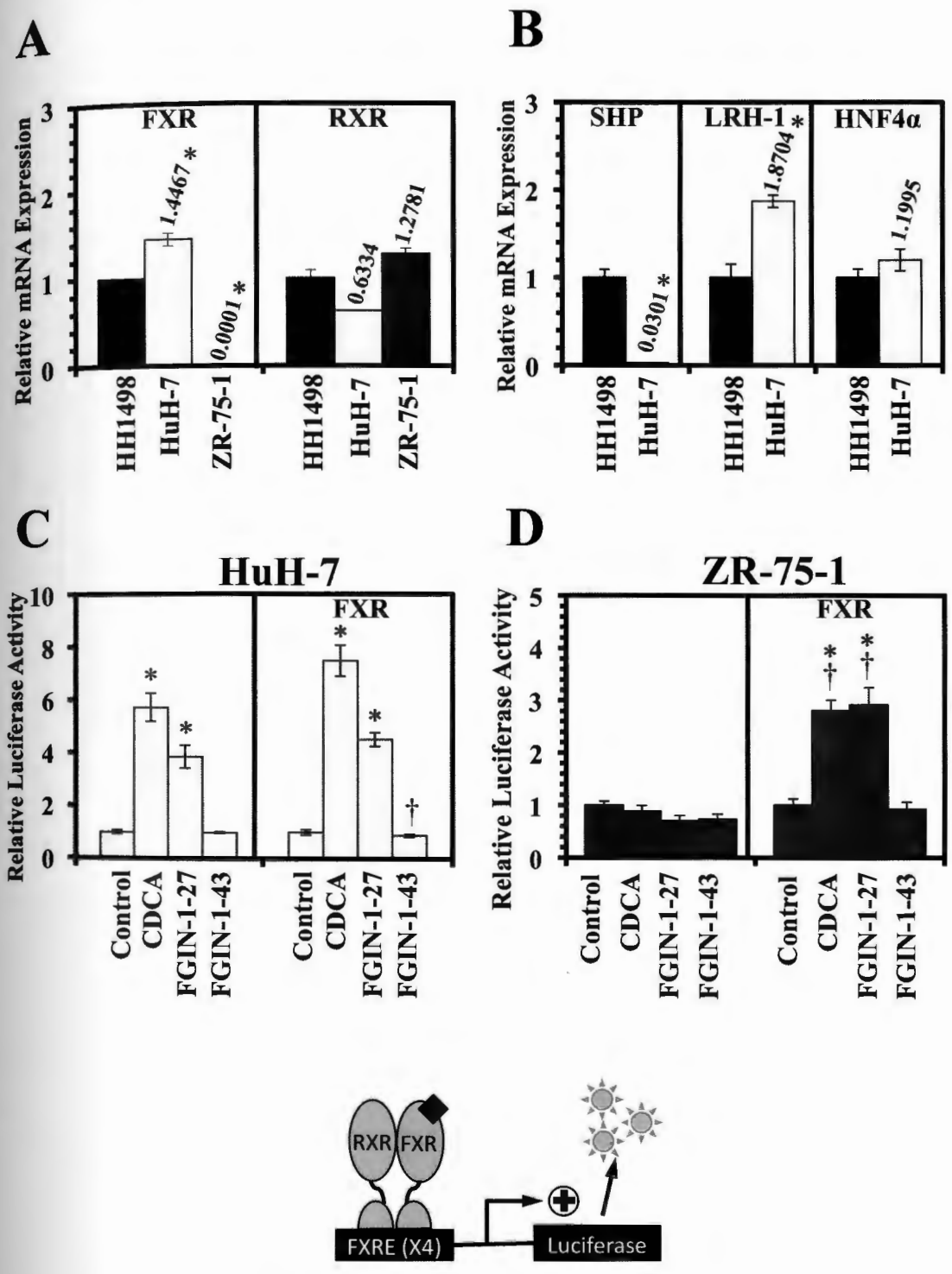
A
FXR
RXR
Relative mRNA Expression
1.4467 *
0.0001 *
0.6334
1.2781
HH1498
HuH-7
ZR-75-1
B
SHP
LRH-1
HNF4α
0.0301 *
1.8704 *
1.1995
C
HuH-7
FXR
Relative Luciferase Activity
Control
CDCA
FGIN-1-27
FGIN-1-43
D
ZR-75-1
RXR
FXR
FXRE (X4)
Luciferase

Figure 6

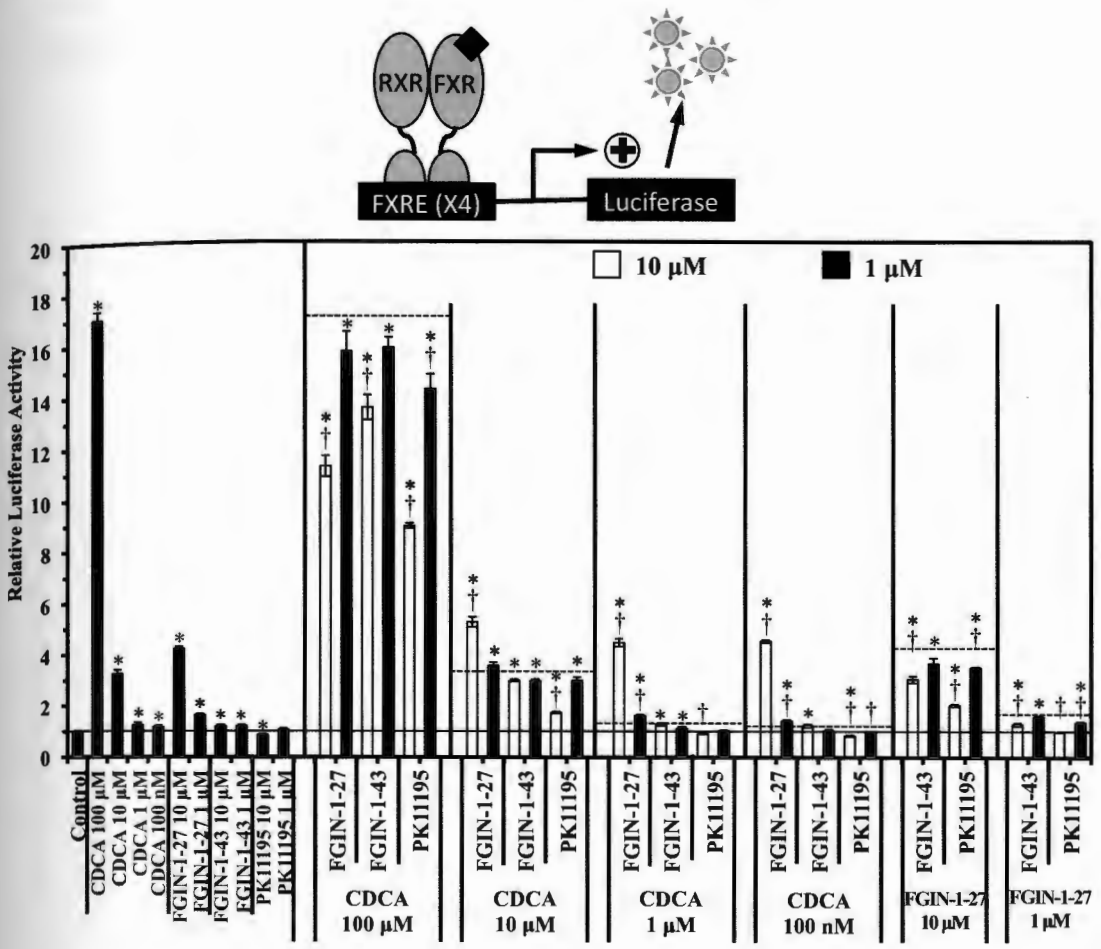
RXR
FXR
FXRE (X4)
Luciferase
10 µM
1 µM
Relative Luciferase Activity
0
2
4
6
8
10
12
14
16
18
20
Control
CDCA 100 µM
CDCA 10 µM
CDCA 1 µM
CDCA 100 nM
FGIN-1-27 10 µM
FGIN-1-27 1 µM
FGIN-1-43 10 µM
FGIN-1-43 1 µM
PK11195 10 µM
PK11195 1 µM
FGIN-1-27
FGIN-1-43
PK11195
CDCA 100 µM
CDCA 10 µM
CDCA 1 µM
CDCA 100 nM
FGIN-1-27 10 µM
FGIN-1-27 1 µM

Figure 7

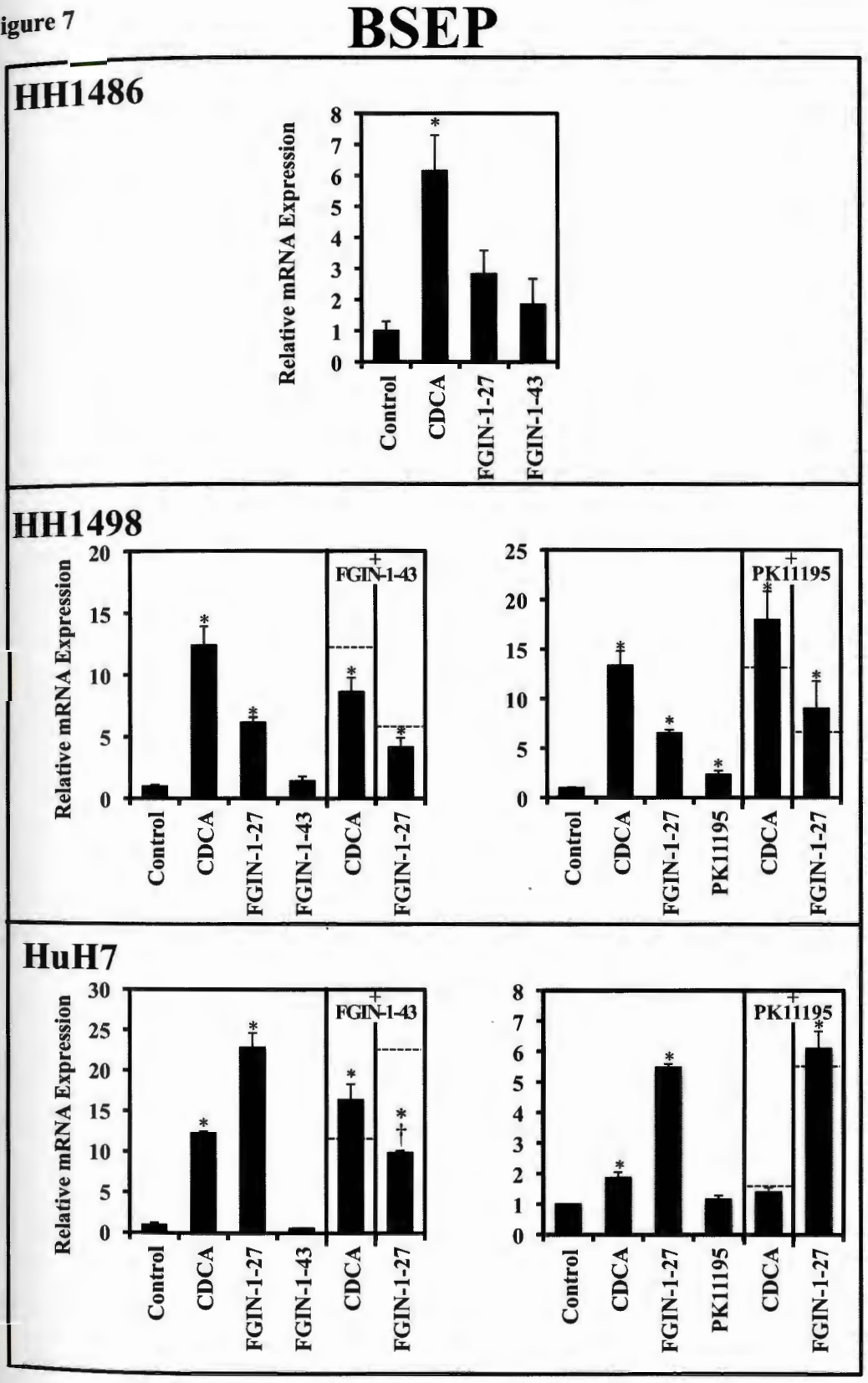
BSEP
HH1486
Relative mRNA Expression
Control
CDCA
FGIN-1-27
FGIN-1-43
HH1498
FGIN-1-43
PK11195
HuH7

Figure 8

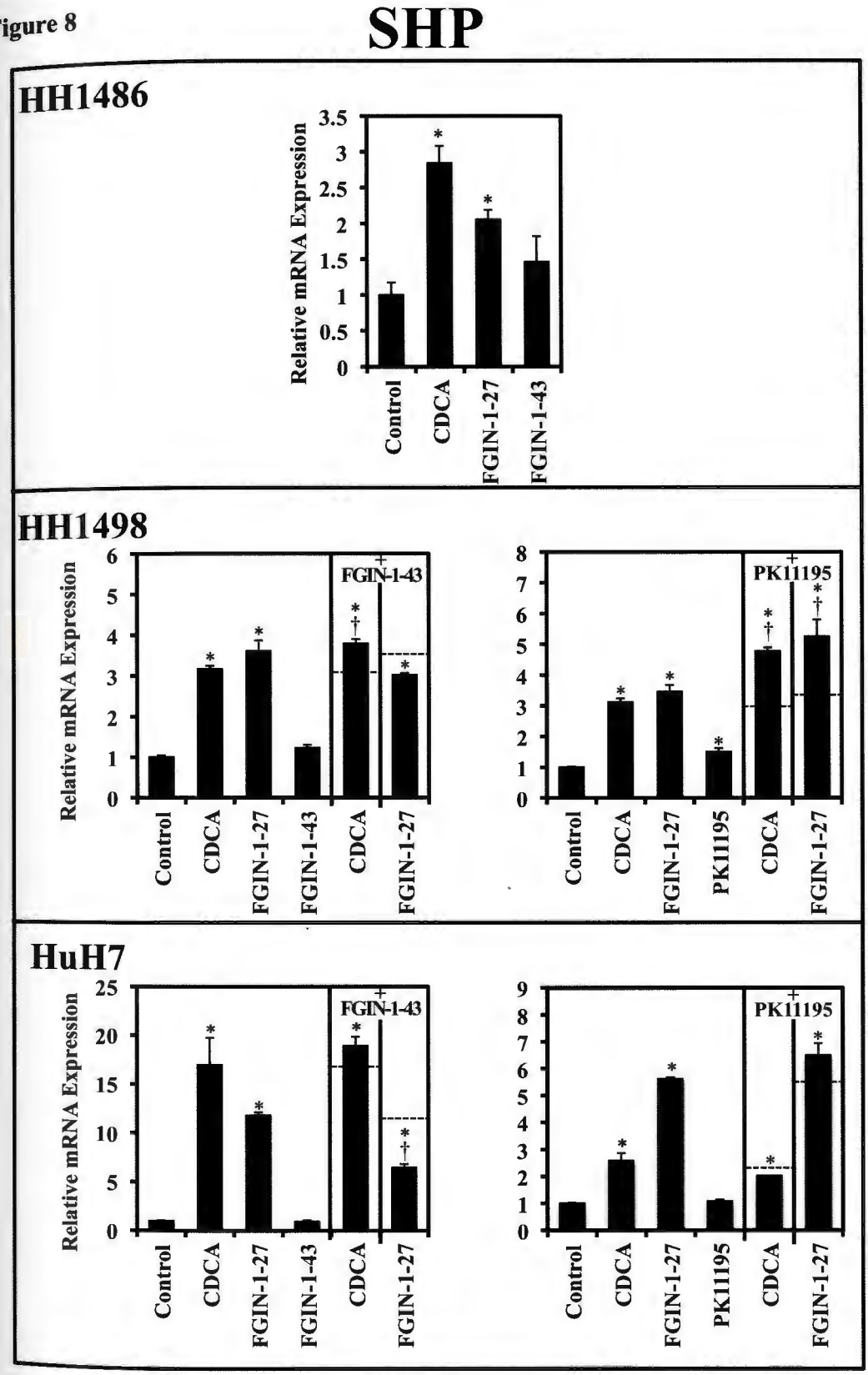
SHP
HH1486
Relative mRNA Expression
3.5
3
2.5
2
1.5
1
0.5
0
Control
CDCA
FGIN-1-27
FGIN-1-43
HH1498
Relative mRNA Expression
FGIN-1-43
Control
CDCA
FGIN-1-27
FGIN-1-43
CDCA
FGIN-1-27
PK11195
Control
CDCA
FGIN-1-27
PK11195
CDCA
FGIN-1-27
HuH7
Relative mRNA Expression
FGIN-1-43
Control
CDCA
FGIN-1-27
FGIN-1-43
CDCA
FGIN-1-27
PK11195
Control
CDCA
FGIN-1-27
PK11195
CDCA
FGIN-1-27

Figure 9

CYP7A1

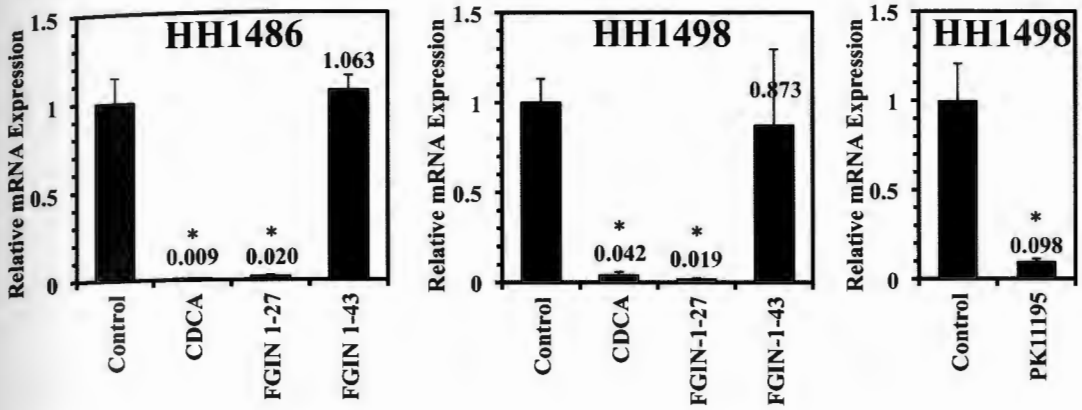

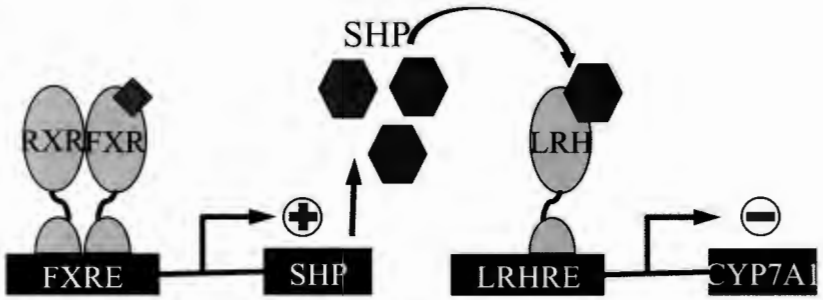

Figure 10

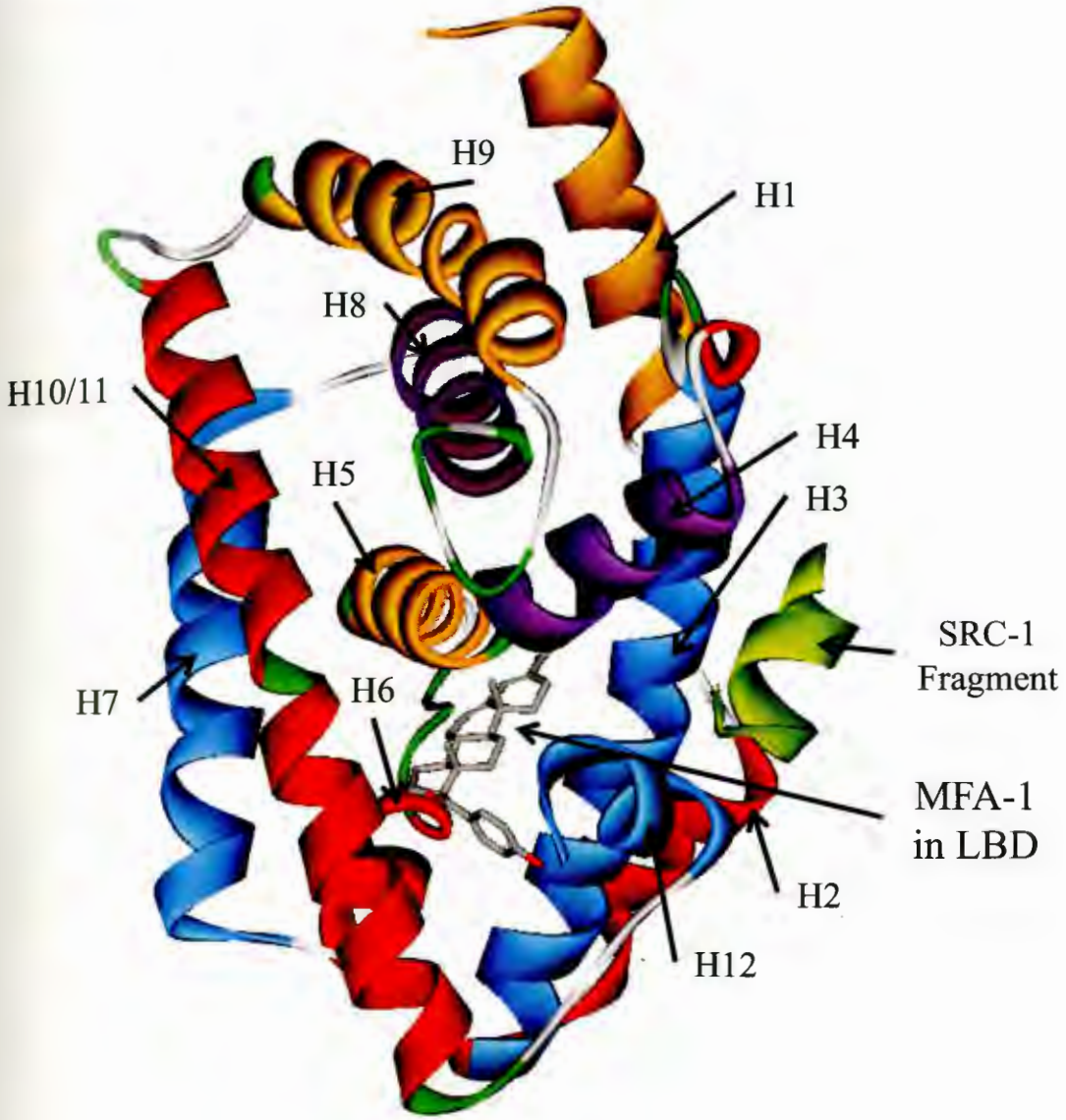

Figure 11 A and B

A

CDCA

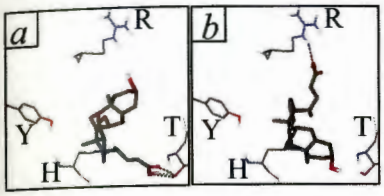

CDCA		
	Binding Energy (kcal/mol)	% frequency
a	-9.7539 ± 0.0086	86.80
b	-9.4465 ± 0.0279	13.20

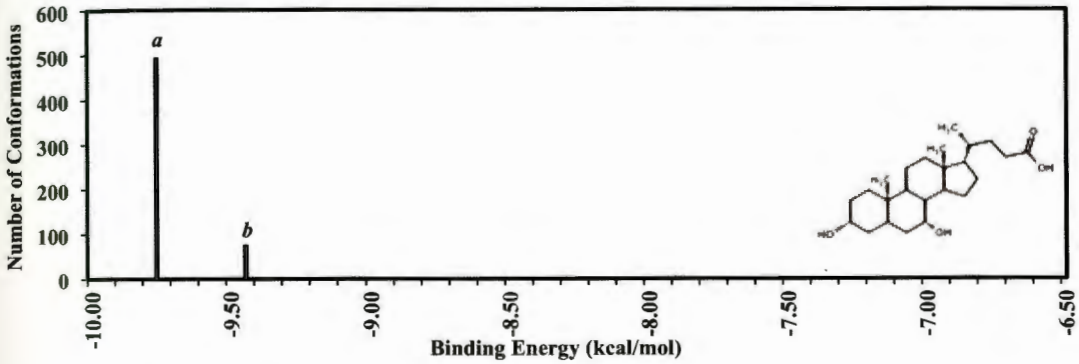

B

FGIN-1-27

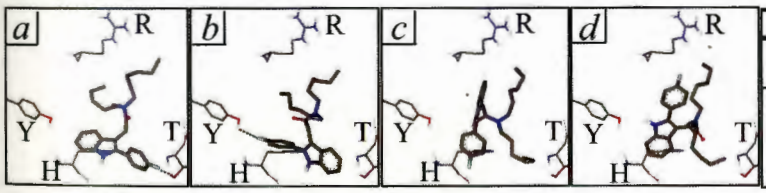

FGIN-1-27		
	Binding Energy (kcal/mol)	% frequency
a	-9.3351 ± 0.0272	41.07
b	-9.1217 ± 0.0547	20.45
c	-8.7669 ± 0.0512	20.13
d	-8.5449 ± 0.0537	18.34

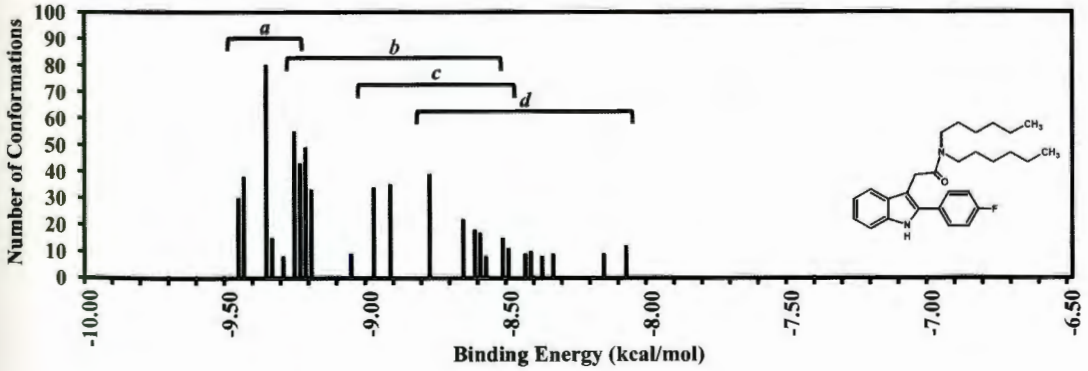

Figure 11 C and D

C

FGIN-1-20

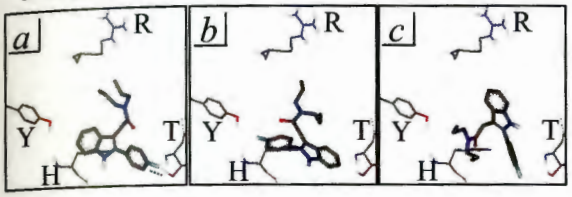

FGIN-1-20		
	Binding Energy (kcal/mol)	% frequency
a	-8.7135 ± 0.0078	59.55
b	-8.9750 ± 0.0277	6.74
c	-9.1083 ± 0.0160	33.71

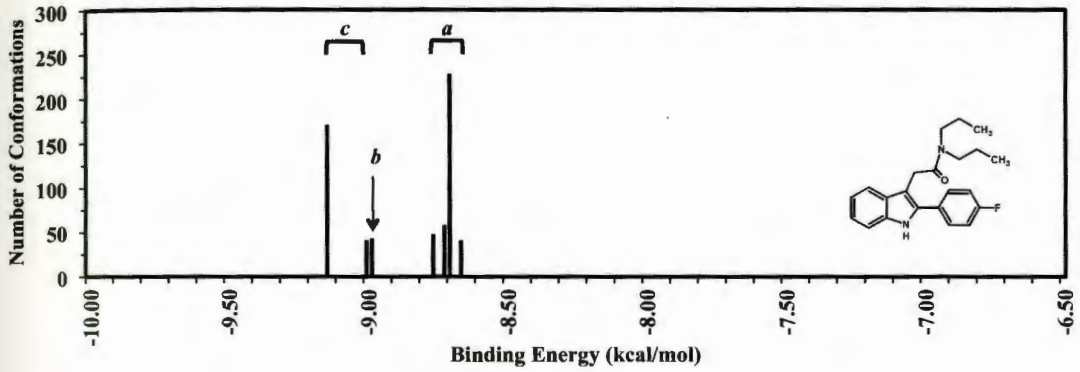

D

FGIN-1-51

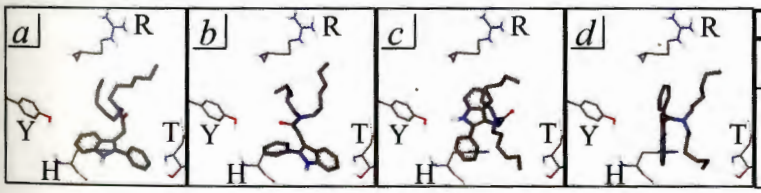

FGIN-1-51		
	Binding Energy (kcal/mol)	% frequency
a	-9.5968 ± 0.0281	39.97
b	-9.3158 ± 0.0428	29.52
c	-9.0519 ± 0.0446	15.09
d	-8.9140 ± 0.0498	15.42

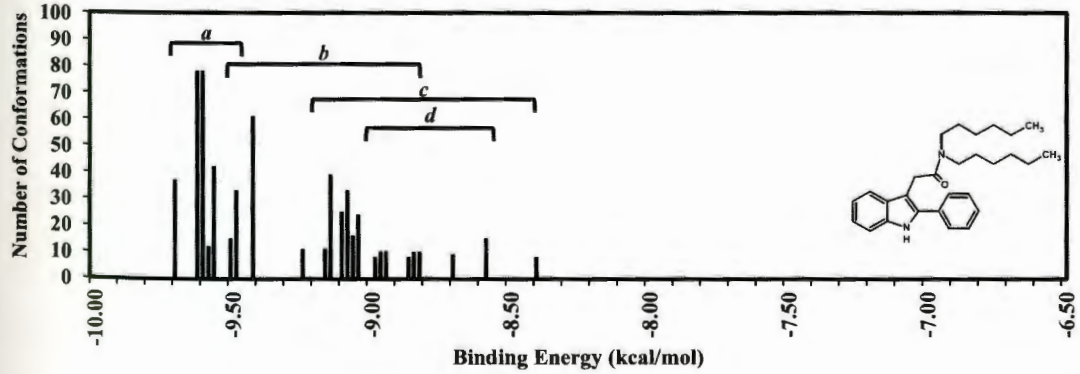

Figure 11 E and F

E

FGIN-1-43

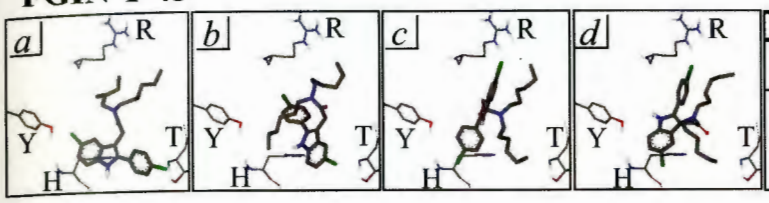

FGIN-1-43		
	Binding Energy (kcal/mol)	% frequency
a	-7.3401 ± 0.1579	15.83
b	-8.1590 ± 0.2076	15.13
c	-8.3377 ± 0.0820	40.35
d	-8.7693 ± 0.1026	28.70

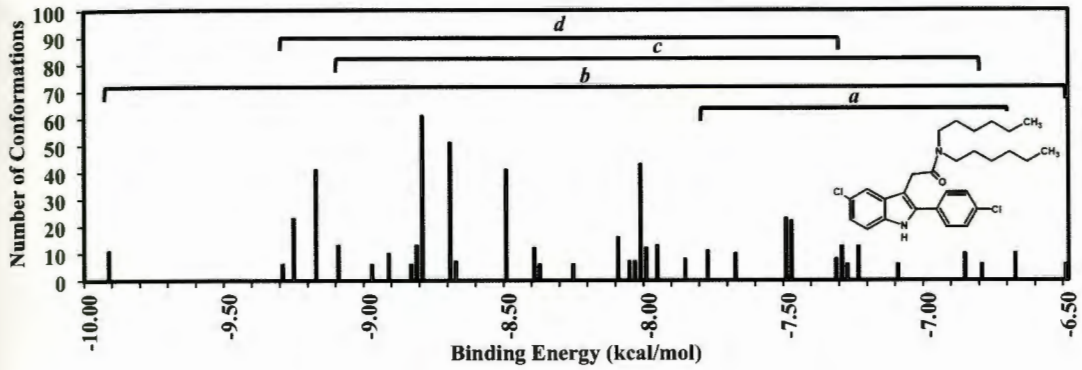

F

PK11195

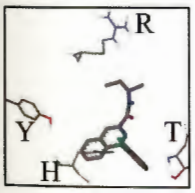

PK11195		
	Binding Energy (kcal/mol)	% frequency
	-9.6416 ± 0.0054	100.00

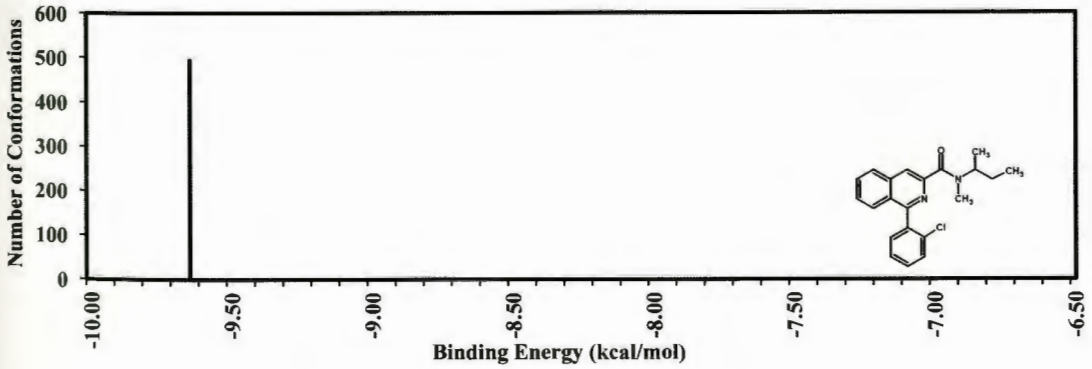

Figure 12

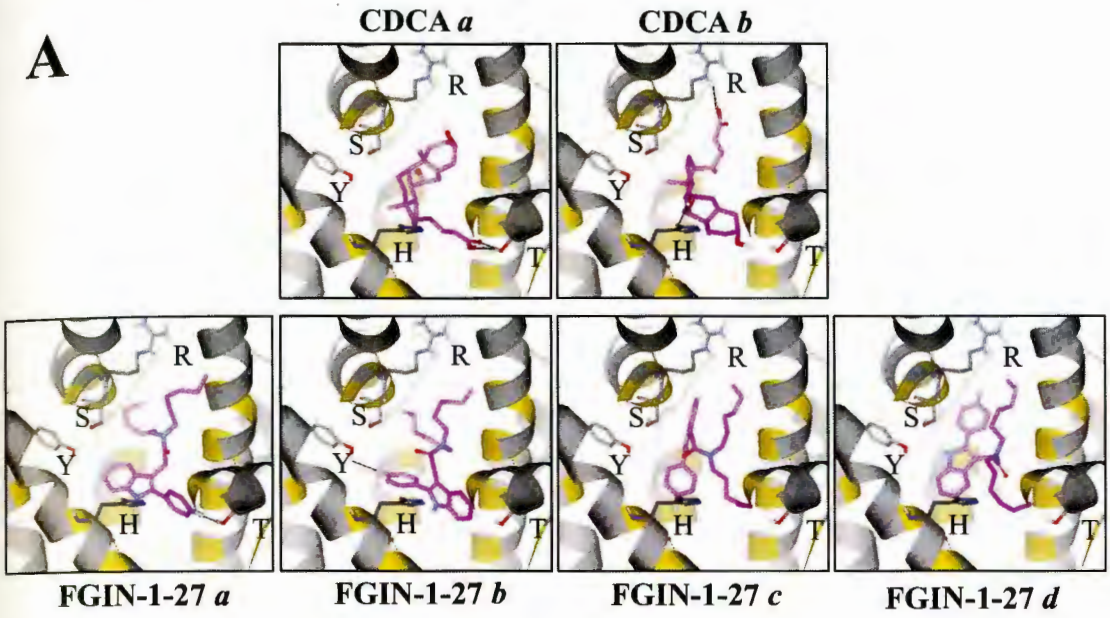
A
CDCA a
CDCA b
R
S
Y
H
T
FGIN-1-27 a
FGIN-1-27 b
FGIN-1-27 c
FGIN-1-27 d

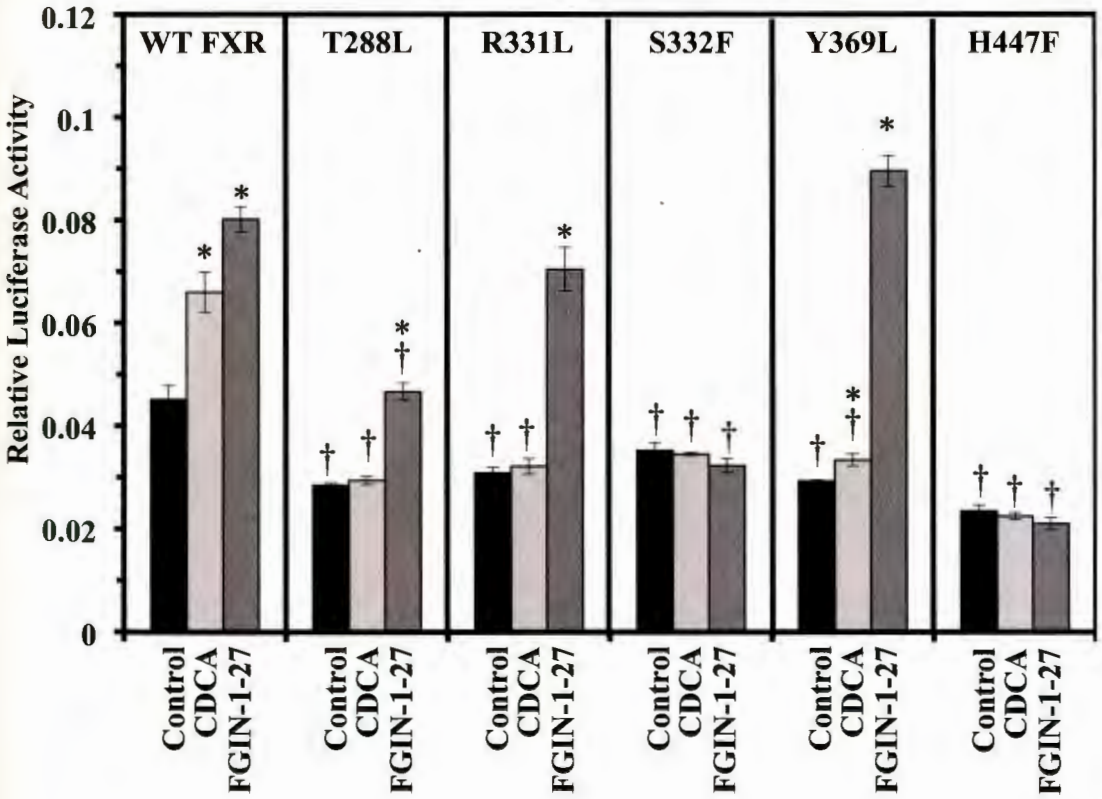
B
Relative Luciferase Activity
0.12
0.1
0.08
0.06
0.04
0.02
0
WT FXR
T288L
R331L
S332F
Y369L
H447F
Control
CDCA
FGIN-1-27

Figure 13

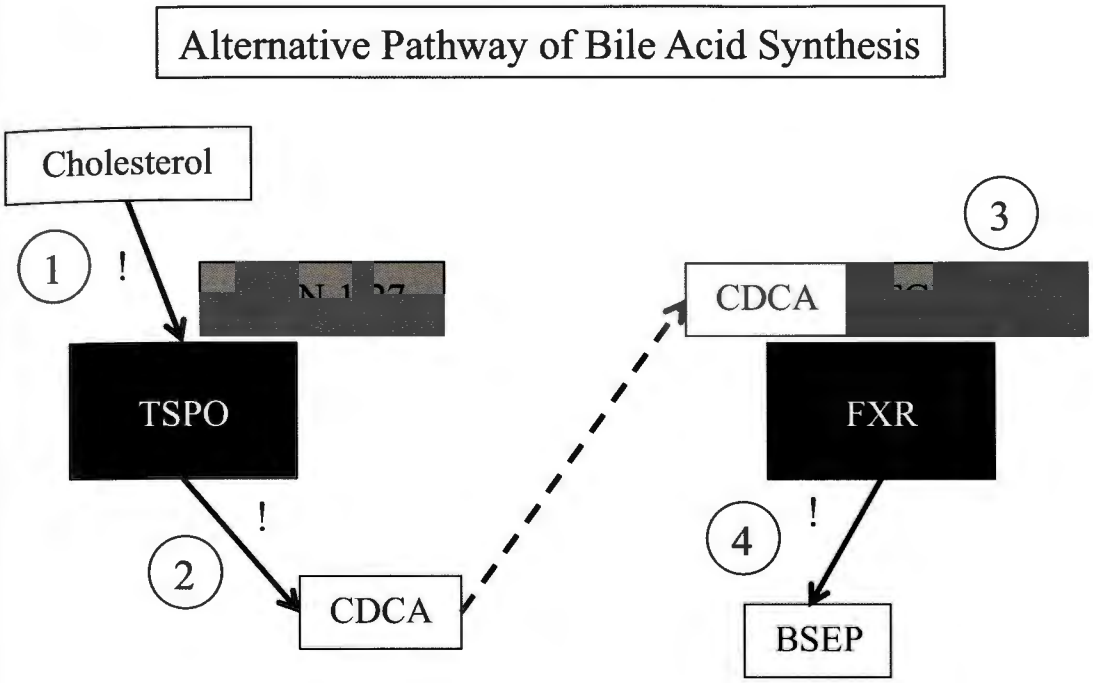
Alternative Pathway of Bile Acid Synthesis
Cholesterol
1
!
TSPO
!
2
CDCA
3
CDCA
FXR
4
!
BSEP